

# VU Research Portal

## Sensing Seasonality by Planktonic Foraminifera

Feldmeijer, W.

2015

### **document version**

Publisher's PDF, also known as Version of record

[Link to publication in VU Research Portal](#)

### **citation for published version (APA)**

Feldmeijer, W. (2015). *Sensing Seasonality by Planktonic Foraminifera*. [, Vrije Universiteit Amsterdam].

### **General rights**

Copyright and moral rights for the publications made accessible in the public portal are retained by the authors and/or other copyright owners and it is a condition of accessing publications that users recognise and abide by the legal requirements associated with these rights.

- Users may download and print one copy of any publication from the public portal for the purpose of private study or research.
- You may not further distribute the material or use it for any profit-making activity or commercial gain
- You may freely distribute the URL identifying the publication in the public portal ?

### **Take down policy**

If you believe that this document breaches copyright please contact us providing details, and we will remove access to the work immediately and investigate your claim.

### **E-mail address:**

[vuresearchportal.ub@vu.nl](mailto:vuresearchportal.ub@vu.nl)



*Globorotalia truncatulinoides*

## Late Pleistocene Glacial-Interglacial related shell size isotope variability in planktonic foraminifera as a function of local hydrology

*B. Metcalfe, W. Feldmeijer, M. de Vringer-Picon, G.-J.A. Brummer, F.J.C. Peeters and G.M. Ganssen*

So called ‘vital effects’, a collective noun for a suite of physiological and metabolic induced variability, in oxygen ( $\delta^{18}\text{O}$ ) and carbon ( $\delta^{13}\text{C}$ ) isotope ratios of planktonic foraminifer shells hamper precise quantitative reconstruction of past ocean parameters. Correction for potential isotopic offsets from the equilibrium or the expected value is paramount, as too is the ability to define a comparable life-stage for each species that allows for direct comparison. Past research has focused upon finding a specific size range for individual species in lieu of other identifiable features, that allow ocean parameters from a particular constant (i.e. a specific depth or season) to be reconstructed. Single shell isotope analysis of fossil shells from a mid-latitude North Atlantic Ocean piston-core covering Termination III (200 kyr to 250 kyr) highlight the advantage of using a dynamic size range in studies of palaeoclimate. Using this methodology, we show that isotopic offsets between specimens in successive size fractions of *G. inflata* and *G. truncatulinoides* are not constant over time, contrary to previous findings. For  $\delta^{18}\text{O}$  in smaller sized globorotalids it is suggested that the offset from other size fractions may reflect a shallower habitat in an early ontogenetic stage. A reduction in the difference between small and large specimens of *G. inflata* between insolation minima and maxima is interpreted to relate to a prolonged period of reduced water column stratification. For the shallow dwelling species *G. bulloides* no size isotope difference between size fractions is observed, and the variability in the oxygen isotopic values are shown to correlate well with the seasonal insolation patterns. As such, patterns in oxygen isotope variability of fossil populations may be used successfully for reconstruction of past seasonality changes.

## 8.1 Introduction

### 8.1.1 Size of planktonic foraminifera

A series of biogeochemical and physical proxies exist to determine the mechanisms of short-term and long-term climate change from archives such as deep sea sediments. Notably amongst these is the isotopic composition of planktonic foraminifera because of the continuous export flux of shells to the ocean floor and their near-global occurrence. The inherent weakness within these proxy archives is that these are neither the original nor the unaltered reflection of the primary signal. Therefore, quantifying the limitations and potential artefacts is imperative for drawing robust conclusions. Deviation from equilibrium values, an isotopic offset caused by biological fractionation commonly referred to as the 'vital effect' likely reflects changes in metabolic processes and rates during shell formation. Previous studies have shown that, in order to minimise or reduce the potential influence of metabolic effects, specimens should be constrained to a similar size and shape [Berger *et al.*, 1978; Billups and Spero, 1995; Bouvier-Soumagnac and Duplessy, 1985; Curry and Matthews, 1981; Elderfield *et al.*, 2002; Friedrich *et al.*, 2012; Kroon and Darling, 1995; Ravelo and Fairbanks, 1992, 1995; Shackleton and Vincent, 1978; Weiner, 1975; Williams *et al.*, 1981]. However, the factors that govern/regulate the biomineralisation process in planktonic foraminifera are currently not implicitly understood, with many studies making no distinction between biocalcification and inorganic precipitation. Weinkauf *et al.* [2013] considered that there is some implied trade-off, with respect to resource allocation between production of biomass and biomineralisation, this would fit with the implicit assumption of the optimum growth hypothesis of de Villiers [2004] which is consistent with size reflecting optimum ecological conditions [Schmidt *et al.*, 2004]. Shell size, in itself, reflects an easily measured parameter with a direct relation between both inherited (genetic) and environmental stimuli (e.g. temperature, availability of food). In practical terms, throughout its life an organism will invariably increase in size until some discrete threshold limit is reached due to either mechanical (i.e. test construction), physiological (i.e. maturation; reproduction) or physical constraints (i.e. abiotic/biotic factors) [Schmidt *et al.*, 2004; 2006; 2008]. Schmidt *et al.* [2006] considered that optimum conditions for planktonic organisms could either lead to rapid reproduction and therefore small body size, or fast growth rates and hence larger sizes. Hecht [1974] demonstrated the latter using North Atlantic core top material, *i.e.* that species of planktonic foraminifera obtain their maximum size in waters that are considered (close to-) optimal for that species, decreasing in size away from this point. Although what is considered optimal for pelagic organisms can be complicated by the fact that optimal conditions can occur both geographically and vertically (water depth) [Telford and Kucera, 2013]. Despite this, as environmental conditions change through time organisms can either adapt to new conditions (*i.e.* plasticity: ecophenotypes) or 'track' their preferred habitat leading to a change in body size, the severity of which is dependent upon the location [Malmgren and Kennett, 1976]. Whilst foraminifera are limited in their ability to track their

preferred habitat, being free-floating members of the plankton, it is likely when transported into favourable environmental conditions growth occurs. The effect of this plasticity of size, and potential growth rate variations, upon stable isotopes is less clear.

*Emiliani's* [1954a] investigation on the isotopic composition of foraminifera of two different sizes (250-500  $\mu\text{m}$  and 500-1000  $\mu\text{m}$ ), in combination with a subsequent study extending this line of enquiry [*Emiliani*, 1971], postulated that this size-isotope relationship could be influenced by a change in depth habitat after finding a difference between samples from glacial and interglacials. Certainly if depth habitats are ultimately constrained by food supply and therefore by the penetrative depth of light, then during glacial, when productivity was high, a reduced transmission of light may have occurred [*Volten et al.*, 1998] thus foraminifera would have undergone an "upward migration" of depth habitats [*Berger et al.*, 1978]. Whilst a depth-habitat ranking based upon large sized specimens would not differ from the general attribution of depth to individual species, this is not the case for smaller sized groups which in general have a warmer and thus shallower signal [*Kahn*, 1978]. Subsequent investigations have contented themselves with using a single depth in core, or core top, to determine the size-isotope relationship at a given geographic location despite these earlier postulations on the contrary.

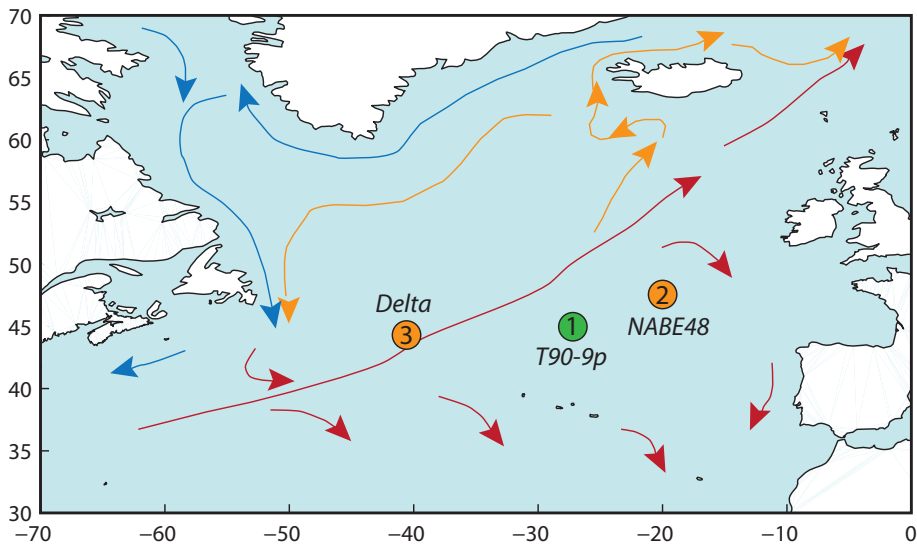


Figure 8.1. Location map of the North Atlantic region. Location map of (1) piston core APNAP T90-9p and long term observation stations (2) sediment trap NABE 48 [*Wolfreich*, 1994] and (3) Ocean Station Delta [*Bé and Tolderlund*, 1971] with main ocean currents overlain, colour indicates relative temperature of the dominant water mass.

1

2

3

4

5

6

7

8

9

R &amp; A

### 8.1.2 Aims and objectives

We here test the sensitivity of shell size to a large-scale environmental perturbances seen at a glacial-interglacial transition, by focusing upon TIII based upon prior research [Chapter 6-7], and further elucidate upon the shell size isotope relationship [Birch *et al.*, 2013; Friedrich *et al.*, 2012] via single shell stable isotope analysis [Ganssen *et al.*, 2011 and references therein]. Specimens are from a section of JGOFS APNAP core T90-9p (45°17.5'N 27°41.3'W; core length = 1028 cm, Figure 8.1), recovered from the eastern flank of the Mid-Atlantic Ridge, in

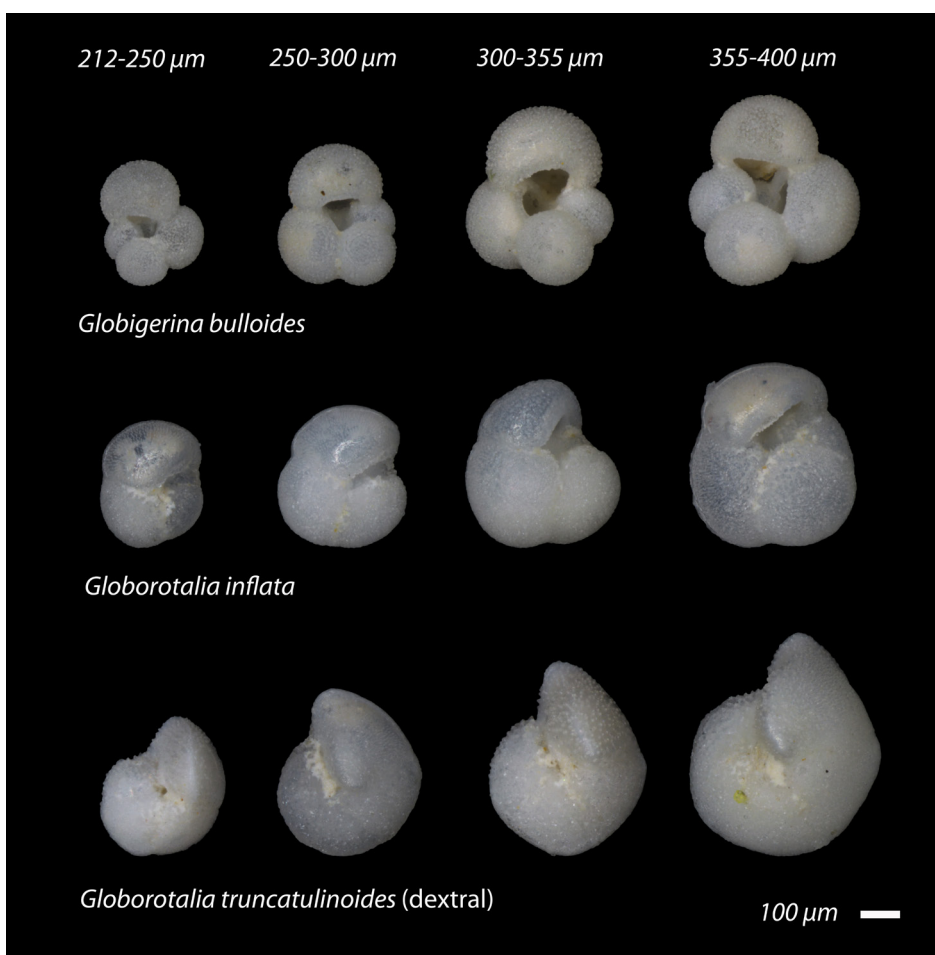


Figure 8.2. Taxonomy and size of species analysed in this paper. Apertural view of (Top) the ‘surface dweller’ *Globigerina bulloides*, (Middle) ‘intermediate dweller’ *Globorotalia inflata* and (Bottom) the ‘deep dweller’ *Globorotalia truncatulinoides* for the following size fractions: 212-250  $\mu\text{m}$ , 250-300  $\mu\text{m}$ , 300-355  $\mu\text{m}$  and 355-400  $\mu\text{m}$  from a 756 cm depth in core. Scale bar (100  $\mu\text{m}$ ) is the same for all images, highlighting the offset between the various size fractions.

the North Atlantic Ocean [Lototskaya and Ganssen, 1999; Lototskaya et al., 1998; Chapter 6-7]. Data on small (212-250  $\mu\text{m}$ ) and large (355-400  $\mu\text{m}$ ) specimens of dextral and sinistral *Globorotalia truncatulinoides* have been reported elsewhere [Chapter 7]. Planktonic foraminifera collected from sediments form the basis of palaeoceanographic reconstructions, usually through  $\delta^{18}\text{O}$  and  $\delta^{13}\text{C}$  on a group of specimens. If such an analysis were repeated several times, then the variability seen would be expected to be smaller compared with the variability one would obtain if specimens were measured individually. This variability is expected to decrease with the reciprocal value of the square root of the number of specimens within a single analysis. In other words, using this method, the variability is reduced for the sake of eliminating noise that may otherwise unduly influence time series analysis. The isotopic information within single specimens is however lost. Given the dynamic nature of the ocean, individuals collected together in a single sedimentary sample may have calcified in different seasons (or years), at different depths, or even in different water masses. Intra and inter specific variability in isotopes have been used to explain either upper ocean processes such as (1) calcification depth changes [Emiliani, 1954a]; (2) variations in metabolism through ontogeny [Killingley et al., 1981; Vergnaud-Grazzini, 1976; Rink et al., 1998] and/or bottom water processes: (3) bioturbation and benthic organism interaction [Bard, 2001; Bard et al., 1987; Löwemark et al., 2008; Wit et al., 2013] and (4) dissolution/recrystallisation [Bonneau et al., 1980]. Given that the life cycle of upper ocean dwelling species is probably completed within a few weeks [Bé et al., 1977; Berger, 1969a], and that a single chamber is formed over a few hours single shell analysis allows us to glimpse at short-term conditions in the ocean [Killingley et al., 1981]. The transition from Marine Isotope Stage (MIS) 8 to 7 at around 232 kyr (Termination III), studied here is generally characterized by a reduced amplitude in oxygen isotope values compared with other glacial terminations, as the preceding cold stage (MIS 8) is muted, with only a reported shift of  $\sim 1.1\text{‰}$  in benthic foraminiferal  $\delta^{18}\text{O}$ . MIS 7 is composed of three warm (MIS 7 substages MIS 7a, MIS 7c and MIS 7e) and two cold phases (MIS 7 substages MIS 7b and MIS 7d) [Roucoux et al., 2006] with the termination characterised by relatively high eccentricity and hence by a heightened difference in the maximum seasonal insolation as defined by the difference between the maximum and minimum insolation during the year [Berger et al., 2006].

## 8.2 Methodology

### 8.2.1 Calculation of average size and weight

Abundance counts of foraminifera were performed at four cm resolution on sediment that was wet sieved over a 63  $\mu\text{m}$  mesh size, dried, passed over a nest of sieves of 125  $\mu\text{m}$ , 212  $\mu\text{m}$ , 250  $\mu\text{m}$ , 300  $\mu\text{m}$ , 355  $\mu\text{m}$  and 400  $\mu\text{m}$  mesh size and the resultant dry residues were weighed. The dried residues were split into small aliquots approximately containing two hundred particles and the number of *Globigerina bulloides*, *Globorotalia inflata* and *Globorotalia truncatulinoides* (Figure 8.2) were counted. Counts were subsequently converted into numbers



R & A



per gram by multiplying the absolute number by the split and the size frequency distribution (SFD) approximated, following the methodology of *Peeters et al.* [1999].

### 8.2.2 Stable isotope geochemistry ( $\delta^{18}\text{O}$ )

Bulk measurements routinely consist of between 8–40 specimens which depending on the species represent ~0.3–1.50 mg of calcium carbonate per sample [*Waelbroeck et al.*, 2005]. Sample preparation in combination with improved mass spectrometry techniques now allows for measurement of single shells down to a few micrograms [*Ganssen et al.*, 2011], or even analysis to the level of individual chambers [*Kozdon et al.*, 2009; *Vetter et al.*, 2013] depending on analytical methodology followed. This constitutes an improvement by a factor of 10–1000 compared to the early pioneering studies of *Emiliani* [1955] and *Shackleton* [1965]. Specimens of *G. bulloides*, *G. inflata* and *G. truncatulinoides* were analysed singularly with about 20 individuals picked from each of four successive size fractions (212–250  $\mu\text{m}$ ; 250–300  $\mu\text{m}$ ; 300–355  $\mu\text{m}$  and 355–400  $\mu\text{m}$ ) following ultrasonic cleaning in ethanol. Analysis was conducted on a Thermo Finnigan Delta<sup>+</sup> mass spectrometer equipped with a GASBENCH II preparation device. In order to analyse individual specimens, ranging in weight between 5–50  $\mu\text{g}$ , samples are placed in He-filled 3 ml exetainer vial with a set of glass beads (~2 mm). The beads act both as a heat buffer and as a preventative measure against loss upon contact with the acid, a problem that is generally overcome when measuring in groups. Each sample is digested in concentrated phosphoric acid ( $\text{H}_3\text{PO}_4$ ) at 45 °C. Isotope values are reported as  $\delta^{18}\text{O}$  and  $\delta^{13}\text{C}$  versus Vienna Pee Dee Belemnite (V-PDB) calculated using the standard delta notation ( $\delta$ ) and reported in per mil (‰). The reproducibility of routinely analysed laboratory calcium carbonate standards is better than 0.12 ‰ (1 $\sigma$ ) for both  $\delta^{18}\text{O}$  and  $\delta^{13}\text{C}$ , given the heterogeneity of carbonate standards at this critical low concentration of material analysed [*Ishimura et al.*, 2008]. This represents ~5 % of the measured range and therefore is considered negligible.

### 8.2.3 Statistical Analysis

Single specimen analysis allows for a more stringent battery of statistical tests to be carried out than “traditional”, grouped, analysis. We follow methodological procedures described in *Ganssen et al.* [2011], in which the individual datasets (multiple analyses of single specimens from one size fraction) are checked for potential outliers in order to both produce a robust estimate of the range and the mean (Table 8.1 and 8.2). Lower and upper bound were calculated using the first quartile ( $Q_1$ ), third quartile ( $Q_3$ ) and the interquartile range (IQR). This does however remove the extremes in  $\delta^{18}\text{O}_c$  – and potential minima and maxima in temperature – yet in order to compare size fractions using a student t-distribution based confidence interval the calculated mean must be robust. Whilst no dataset fits the normal distribution, distributions that approximate the normal distribution are considered to be unimodal with the measures of central



## Size-isotope relationship in planktonic foraminifera

Oxygen isotope ( $\delta^{18}O$ )

Shaded columns represent samples that were determined to be not normally distributed. Outliers were removed from this dataset

Species	Size fraction ( $\mu m$ )	Specimen no.	729	732	736	740	744	748	752	756	760	764	768	772	776	780	784	788	792	796	800	804	808	812	816	820	824	828		
<i>G. bulloides</i>	212	250	1	1.916	1.734	0.815	1.452	1.509	1.564	1.585	2.359	1.817	0.507	1.504	1.434	0.810	1.747	1.127	1.123	0.507	2.001	2.312	2.652	2.689	2.310	1.602	1.715	2.996		
<i>G. bulloides</i>	212	250	2	1.203	2.032	0.551	0.039	2.247	1.815	0.235	1.719	1.334	0.860	0.035	1.435	0.532	1.876	0.483	0.956	2.508	2.767	2.888	2.487	1.730	1.477	2.889	1.326	1.564		
<i>G. bulloides</i>	212	250	3	0.881	1.167	1.217	0.311	0.628	2.197	1.033	1.340	0.196	1.327	1.989	1.980	1.132	0.705	0.969	0.297	1.958	2.136	2.041	1.977	1.456	1.928	1.924	1.167	2.554		
<i>G. bulloides</i>	212	250	4	0.908	0.993	0.324	1.783	1.383	1.241	1.711	1.124	0.422	1.135	0.237	0.032	1.028	1.159	0.388	1.326	2.028	1.970	2.088	1.714	1.721	1.568	1.369	2.754	2.326	2.827	
<i>G. bulloides</i>	212	250	5	1.376	1.024	0.124	1.783	1.383	1.241	1.711	1.124	0.422	1.135	0.237	0.032	1.028	1.159	0.388	1.326	2.028	1.970	2.088	1.714	1.721	1.568	1.369	2.754	2.326	2.827	
<i>G. bulloides</i>	212	250	6	0.886	0.990	1.346	0.007	1.054	0.880	0.498	1.992	1.449	0.222	0.458	0.952	0.807	1.187	0.733	1.529	1.704	2.027	2.029	1.971	2.384	1.347	1.464	1.306	1.933	1.713	
<i>G. bulloides</i>	212	250	7	1.513	1.150	0.738	-0.423	0.290	2.704	0.838	2.153	1.618	1.699	1.260	2.204	1.635	-0.253	-1.198	1.482	1.992	1.418	2.319	2.337	2.033	0.915	1.503	2.703	1.566	2.435	
<i>G. bulloides</i>	212	250	8	0.749	2.309	2.699	-0.602	0.299	2.172	0.923	0.498	1.992	1.449	0.222	0.458	0.952	0.807	1.187	0.733	1.529	1.704	2.027	2.029	1.971	2.384	1.347	1.464	1.306	1.933	1.713
<i>G. bulloides</i>	212	250	9	1.239	1.238	0.958	1.581	2.597	1.229	1.253	1.428	1.033	0.727	0.888	1.474	0.529	0.807	1.044	1.409	1.203	1.817	1.862	1.802	1.433	0.912	1.503	2.509	2.338	0.945	
<i>G. bulloides</i>	212	250	10	0.880	1.272	0.081	-0.429	0.565	1.731	1.270	1.099	1.362	0.329	0.282	-0.763	0.978	1.328	0.213	1.058	2.440	1.378	2.301	1.959	2.308	1.987	2.682	1.744	2.398	2.468	
<i>G. bulloides</i>	212	250	11	0.906	1.363	0.764	0.786	-0.508	1.787	2.041	1.392	1.609	1.404	0.587	2.184	0.449	0.861	0.179	1.460	1.851	2.884	2.489	2.438	2.294	1.862	1.766	2.784	0.625	2.654	
<i>G. bulloides</i>	212	250	12	1.855	0.698	1.213	0.729	0.069	1.899	2.193	0.810	1.624	1.648	0.486	-0.543	0.620	0.220	0.226	1.088	1.265	2.686	1.057	-0.208	0.544	1.658	1.130	2.323	2.233	2.233	
<i>G. bulloides</i>	212	250	13	-0.325	0.628	1.073	1.162	0.233	0.727	1.187	1.887	0.319	1.042	1.741	0.363	0.559	1.649	1.688	2.493	2.814	2.310	2.276	1.401	0.288	0.907	1.928	0.483	2.397	2.397	
<i>G. bulloides</i>	212	250	14	1.990	1.382	2.419	0.857	0.426	1.775	0.934	2.706	1.737	0.815	1.844	-0.848	0.066	0.243	2.579	2.430	2.584	2.203	2.201	1.738	0.908	0.706	1.131	2.865	2.865		
<i>G. bulloides</i>	212	250	15	0.610	1.101	1.351	0.867	0.677	1.838	1.608	1.675	1.627	1.407	-0.065	1.327	0.255	1.291	2.241	2.263	3.340	1.379	2.560	1.734	0.306	1.764	0.920	1.232	2.441		
<i>G. bulloides</i>	212	250	16	0.746	1.343	2.490	0.461	1.521	1.289	0.956	1.621	1.523	1.089	0.956	1.466	0.486	0.980	0.362	2.340	2.485	2.121	2.542	1.453	1.308	1.489	1.048	1.348	3.097		
<i>G. bulloides</i>	212	250	17	1.001	0.714	1.001	0.714	1.001	0.714	1.001	0.714	1.001	0.714	1.001	0.714	1.001	0.714	1.001	0.714	1.001	0.714	1.001	0.714	1.001	0.714	1.001	0.714	1.001	0.714	
<i>G. bulloides</i>	212	250	18	0.587	1.001	0.714	1.001	0.714	1.001	0.714	1.001	0.714	1.001	0.714	1.001	0.714	1.001	0.714	1.001	0.714	1.001	0.714	1.001	0.714	1.001	0.714	1.001	0.714	1.001	
<i>G. bulloides</i>	212	250	19	0.587	1.001	0.714	1.001	0.714	1.001	0.714	1.001	0.714	1.001	0.714	1.001	0.714	1.001	0.714	1.001	0.714	1.001	0.714	1.001	0.714	1.001	0.714	1.001	0.714	1.001	
<i>G. bulloides</i>	212	250	20	0.587	1.001	0.714	1.001	0.714	1.001	0.714	1.001	0.714	1.001	0.714	1.001	0.714	1.001	0.714	1.001	0.714	1.001	0.714	1.001	0.714	1.001	0.714	1.001	0.714	1.001	
<i>G. bulloides</i>	250	300	1	0.750	0.842	1.474	1.846	1.723	3.099	2.004	2.307	1.616	0.902	0.908	0.419	1.496	1.624	0.564	1.184	1.709	1.594	1.076	2.378	2.425	2.344	1.760	1.979	1.894	2.223	
<i>G. bulloides</i>	250	300	2	1.287	0.808	1.961	1.014	1.951	0.639	1.211	3.156	2.834	1.401	1.035	2.242	1.740	0.486	0.753	0.772	0.598	2.454	2.308	3.225	2.445	2.068	1.721	1.207	1.344	2.654	
<i>G. bulloides</i>	250	300	3	1.375	2.199	0.415	1.165	2.433	2.767	1.269	1.587	1.367	1.004	0.099	1.791	1.230	0.987	1.231	2.271	2.370	2.687	2.592	2.682	2.684	1.987	2.586	2.481	2.228	2.228	
<i>G. bulloides</i>	250	300	4	1.453	1.732	1.169	0.589	2.333	2.337	0.613	2.716	0.601	1.241	2.496	1.026	0.922	0.222	1.677	0.880	1.044	2.541	1.571	2.547	2.429	3.029	1.999	2.411	2.326	2.326	
<i>G. bulloides</i>	250	300	5	1.483	2.068	0.638	1.822	0.638	1.842	1.209	1.787	1.211	1.635	-0.146	1.187	0.762	1.347	1.446	1.129	2.615	2.644	2.901	1.544	1.358	1.169	2.416	2.398	2.416	2.398	
<i>G. bulloides</i>	250	300	6	1.554	1.200	1.121	0.881	0.963	2.565	1.724	2.489	0.854	1.409	1.678	1.605	0.882	1.945	1.701	2.366	2.191	2.588	1.988	3.621	2.321	2.363	2.405	2.620	1.624	1.624	
<i>G. bulloides</i>	250	300	7	1.600	1.801	1.667	1.424	2.687	1.074	2.599	1.972	1.704	2.007	1.042	0.717	-1.053	-0.599	1.460	2.209	2.832	0.989	2.333	2.697	2.431	1.881	1.078	1.759	1.304	3.706	
<i>G. bulloides</i>	250	300	8	1.692	0.835	2.553	2.318	0.850	1.244	1.462	1.517	1.516	2.209	1.943	0.777	-0.180	1.305	2.182	2.827	2.071	2.827	2.827	2.827	2.827	2.827	2.827	2.827	2.827	2.827	
<i>G. bulloides</i>	250	300	9	1.252	0.877	1.411	2.516	2.026	2.304	1.596	1.752	1.966	1.801	1.882	1.154	-1.194	0.883	0.351	2.537	2.088	2.642	2.351	1.975	1.872	1.363	1.312	2.663	2.783	2.783	
<i>G. bulloides</i>	250	300	10	0.686	-0.189	1.050	1.788	2.521	0.484	1.379	0.675	1.189	1.787	2.057	0.984	0.465	-0.137	2.388	1.165	2.303	2.425	2.751	2.335	2.134	2.063	1.801	1.965	2.444	2.444	
<i>G. bulloides</i>	250	300	11	1.179	1.912	1.136	0.938	1.806	2.787	1.736	1.877	1.836	1.032	1.174	1.18	0.857	0.044	2.229	2.499	2.581	2.444	1.308	2.053	1.472	1.363	1.113	1.343	2.053	2.053	
<i>G. bulloides</i>	250	300	12	1.277	0.832	1.034	1.258	2.472	2.778	2.270	1.738	1.412	0.430	0.033	0.748	0.468	0.738	0.528	1.760	2.478	2.531	2.338	2.338	2.338	2.338	2.338	2.338	2.338	2.338	
<i>G. bulloides</i>	250	300	13	1.309	1.219	1.113	0.684	0.765	2.008	1.659	1.659	1.659	1.659	1.659	1.659	1.659	1.659	1.659	1.659	1.659	1.659	1.659	1.659	1.659	1.659	1.659	1.659	1.659	1.659	
<i>G. bulloides</i>	250	300	14	1.212	1.163	0.409	2.843	2.900	2.454	1.014	1.365	3.077	1.489	0.338	1.405	0.338	1.405	0.338	1.405	0.338	1.405	0.338	1.405	0.338	1.405	0.338	1.405	0.338	1.405	0.338
<i>G. bulloides</i>	250	300	15	0.769	2.749	2.749	2.749	2.749	2.749	2.749	2.749	2.749	2.749	2.749	2.749	2.749	2.749	2.749	2.749	2.749	2.749	2.749	2.749	2.749	2.749	2.749	2.749	2.749	2.749	
<i>G. bulloides</i>	250	300	16	1.110	0.886	2.262	2.271	0.846	2.969	1.097	1.588	1.219	1.999	1.553	1.416	0.758	2.813	0.905	0.957	2.842	1.864	2.317	2.126	2.473	1.380	1.872	2.095	1.819	2.095	
<i>G. bulloides</i>	250	300	17	0.659	2.062	2.978	2.958	2.240	2.748	2.978	1.735	1.611	1.738	1.478	1.143	1.980	2.120	2.643	1.889	0.774	2.772	2.282	1.363	2.116	1.512	1.008	2.983	2.983	2.983	
<i>G. bulloides</i>	250	300	18	1.801	1.359	1.050	1.551	2.306	0.886	1.887	2.160	1.887	2.160	1.887	2.160	1.887	2.160	1.887	2.160	1.887	2.160	1.887	2.160	1.887	2.160	1.887	2.160	1.887	2.160	
<i>G. bulloides</i>	250	300	19	-0.027	1.439	1.713	1.461	1.734	1.812	2.625	1.540	1.263	0.904	1.680	1.263	0.904	1.680	1.263	0.904	1.680	1.263	0.904	1.680	1.263	0.904	1.680	1.263	0.904	1.680	
<i>G. bulloides</i>	250	300	20	-0.027	1.439	1.713	1.461	1.734	1.812	2.625	1.540	1.263	0.904	1.680	1.263	0.904	1.680	1.263	0.904	1.680	1.263	0.904	1.680	1.263	0.					

<i>G. inflata</i>	300	355	14	1.806	1.741	1.603	1.149	1.728	2.449	2.359	2.2148	1.303	2.527	1.746	1.927	1.787	1.228	1.441	1.369	1.668	1.9	2.636	1.948	2.474	2.438	2.021	1.089	1.958	1.947			
<i>G. inflata</i>	300	355	16	1.699	1.778	1.781	1.733	1.618	2.356	2.191	1.9846	2.068	2.281	2.084	2.028	1.58	1.43	1.43	1.43	1.43	1.43	1.43	1.43	1.43	1.43	1.43	1.43	1.43	1.43			
<i>G. inflata</i>	300	355	16	1.961	1.389	1.445			2.065	2.166	2.448	1.867	1.566	1.816	2.039	1.468	0.878					1.938	2.235	2.092	2.652	2.615	1.66	2.287	1.698	2.072	1.701	
<i>G. inflata</i>	300	355	17	1.828					2.015	2.054	2.448	1.867	1.566	1.816	2.039	1.468	0.878	0.771	3.47				2.472	1.672	2.313	1.955	1.68	1.755	1.937	2.271	1.711	
<i>G. inflata</i>	300	355	18	2.546								1.4689										2.14	2.262	2.475	2.1	2.441	1.7	2.441	1.7	2.441		
<i>G. inflata</i>	300	355	19	2.06																		1.884	2.487	2.054	1.698	1.963	2.73			2.054		
<i>G. inflata</i>	300	355	20	1.555																		2.321										
<i>G. inflata</i>	355	400	1	1.512	1.744	1.302	1.459	1.94	2.429	2.782	1.588	2.062	1.545	2.046	1.526	1.927	1.087	2.058	1.601	2.145	2.983	2.455	2.544	2.751	2.617	2.605	1.977	1.871	2.395	2.775	2.775	
<i>G. inflata</i>	355	400	2	1.777	1.095	1.166	2.047	1.898	2.007	1.937	2.138	2.007	1.937	2.138	2.007	1.937	2.138	2.007	1.937	2.138	2.007	1.937	2.138	2.007	1.937	2.138	2.007	1.937	2.138	2.007	1.937	
<i>G. inflata</i>	355	400	3	1.855	1.595	2.014	1.641	2.285	2.055	2.431	1.758	2.589	2.51	1.797	1.342	1.707	1.167	1.767	2.822	2.077	2.166	2.089	2.314	2.001	2.62	2.903	2.448	2.248	2.364	2.776	2.776	
<i>G. inflata</i>	355	400	4	1.754	1.519	2.023	1.524	1.962	1.763	2.156	1.808	2.543	2.281	1.795	2.021	1.137	1.873	1.462	2.596	2.531	2.259	2.687	2.502	2.445	2.889	2.889	2.286	2.286	2.603	2.776	2.776	
<i>G. inflata</i>	355	400	5	1.472	1.279	1.535	1.524	1.186	2.055	2.156	1.876	2.491	2.156	1.876	2.491	2.156	1.876	2.491	2.156	1.876	2.491	2.156	1.876	2.491	2.156	1.876	2.491	2.156	1.876	2.491	2.156	
<i>G. inflata</i>	355	400	6	1.549	1.278	1.793	1.722	2.332	2.847	2.565	2.307	2.41	2.059	1.841	1.96	1.833	1.789	1.377	2.658	1.647	2.41	2.68	2.338	2.433	2.443	2.52	2.58	2.845	2.845	2.776	2.776	
<i>G. inflata</i>	355	400	7	1.915	1.489	1.846	1.132	1.813	2.101	2.444	1.708	2.624	2.117	1.388	1.209	1.253	2.384	2.119	2.445	2.384	2.881	2.538	2.407	2.2	2.627	1.738	1.985	2.699	2.62			
<i>G. inflata</i>	355	400	8	1.584	1.832	1.528	1.14	2.262	2.3	2.379	1.738	1.981	2.584	1.405	1.52	1.511	1.862	1.901	2.308	2.212	2.073	2.548	1.984	1.797	2.077	2.548	1.938	2.348	3.012			
<i>G. inflata</i>	355	400	9	1.388	1.281	1.333	1.28	2.499	2.374	1.975	1.5283	2.448	1.616	2.419	1.67	1.102	1.821	1.837	2.401	2.941	2.707	2.711	2.884	2.128	2.985	2.168	2.301	2.392	3.425			
<i>G. inflata</i>	355	400	10	1.746	1.638	1.17	1.975	2.501	2.338	2.288	2.988	1.739	2.349	2.007	1.457	1.352	1.717	1.694	2.330	2.714	3.132	2.644	2.524	2.399	2.501	2.314	1.859	2.819	1.974			
<i>G. inflata</i>	355	400	11	1.282	1.626	1.529	1.841	2.143	1.188	1.914	1.956	2.337	2.223	1.734	1.9	1.35	2.308	2.186	2.805	2.499	2.704	2.902	2.79	2.646	2.381	2.432	1.779	3	2.349			
<i>G. inflata</i>	355	400	12	1.896	1.328	1.417	1.408	2.488	1.986	2.079	2.473	2.263	1.939	1.885	2.396	1.365	1.617	1.893	2.805	2.608	2.625	2.966	2.161	2.304	2.585	2.219	2.798	2.793	1.975			
<i>G. inflata</i>	355	400	13	2.036	1.712	2.243	1.905	2.599	2.791	1.82	2.9078	2.411	1.967	1.847	2.059	1.732	1.184	2.182	1.697	1.75	2.116	2.875	2.755	3.05	2.472	2.008	2.988	2.302	1.588	3.026		
<i>G. inflata</i>	355	400	14	1.385	1.83	1.897	0.988	2.555	2.788	1.577	2.553	2.201	2.431	1.731	1.787	2.055	1.219	1.864	2.289	2.104	2.588	2.081	2.61	2.107	2.708	2.601	2.567	2.704	2.599			
<i>G. inflata</i>	355	400	15	1.623	1.422	1.138	1.492	2.455	1.809	1.499	2.2146	2.484	2.346	1.684	1.865	1.422	1.822	2.027	2.502	2.392	2.509	2.369	2.474	2.318	2.898	2.599	2.338	3.859				
<i>G. inflata</i>	355	400	16	1.696	1.655	2.132	0.958	2.237	2.354	2.149	2.342	2.438	2.189	1.557	1.595	2.05	2.472	2.495	2.405	2.035	2.123	2.41	2.932	2.343	2.619	1.618	2.349	2.619	1.618			
<i>G. inflata</i>	355	400	17	1.796	0.708	1.369	1.951	2.3	1.691	2.281	1.7547	1.87	1.86	1.339	1.224	1.959																
<i>G. inflata</i>	355	400	18	2.128	2.079	1.841	1.847	2.665	2.291	1.855	2.8309	2.429	2.731	1.513	1.604	1.712																
<i>G. inflata</i>	355	400	19	1.544	1.911	1.432	1.399		2.2	2.087	2.1921	1.802	1.572	2.235	1.316																	
<i>G. inflata</i>	355	400	20	1.355	1.657	1.085			2.354	2.373		2.365	1.991																			
<i>G. truncatulinoides</i>	212	250	1	0.66	-0.89	0.758	0.584	-0.012	1.542	1.763	0.0756	1.909	1.812	0.184	0.331	-0.806	-0.296	1.135	1.878	2.042	-0.021	0.925	1.751	0.042	1.135	0.002	0.982	0.384	1.696			
<i>G. truncatulinoides</i>	212	250	2	-0.75	-0.669	0.531	0.2	0.729	1.138	0.869	0.8675	0.232	1.104	1.144	0.454	-0.069	0.116	0.46	0.34	0.995	1.901	1.599	1.098	2.272	1.447	0.958	0.478	-0.404	0.515			
<i>G. truncatulinoides</i>	212	250	3	-0.26	-0.732	0.711	0.16	0.494	1.087	1.671	1.8724	0.643	1.426	0.953	0.27	0.174	-0.109	0.483	0.237	1.05	1.025	1.227	1.363	0.26	1.008	0.603	1.094	0.778	1.567			
<i>G. truncatulinoides</i>	212	250	4	1.75	0.771	-0.652	0.839	0.126	1.282	1.595	1.286	0.982	1.251	0.868	0.431	-0.129	0.304	0.976	1.470	1.511	2.058	1.470	1.511	2.058	1.470	1.511	2.058	1.470	1.511			
<i>G. truncatulinoides</i>	212	250	5	0.068	0.296	0.558	0.064	1.141	0.987	1.628	1.916	1.54	0.958	0.384	0.447	1.065	-0.030	0.173	0.475	0.298	0.448	1.04	1.71	1.833	1.084	-0.787	2.248	1.764	0.798			
<i>G. truncatulinoides</i>	212	250	6	0.245	0.423	-0.103	0.55	0.415	0.343	-0.103	0.55	0.415	0.343	-0.103	0.55	0.415	0.343	-0.103	0.55	0.415	0.343	-0.103	0.55	0.415	0.343	-0.103	0.55	0.415	0.343			
<i>G. truncatulinoides</i>	212	250	7	-0.24	-0.081	-0.181	-0.027	0.401	0.403	0.831	0.837	0.401	0.403	0.837	0.401	0.403	0.837	0.401	0.403	0.837	0.401	0.403	0.837	0.401	0.403	0.837	0.401	0.403	0.837			
<i>G. truncatulinoides</i>	212	250	8	0.627	0.347	0.444	0.221	-0.549	0.423	1.828	0.934	1.173	1.811	-0.115	0.143	-0.43	-0.032	1.11	0.959	0.997	1.248	0.564	1.08	1.287	1.088	0.413	0.742	-0.014	1.2			
<i>G. truncatulinoides</i>	212	250	9	-0.04	-0.262	1.004	-0.105	0.232	0.462	0.865	-0.211	0.818	-0.394	0.254	0.066	-0.925	-0.247	0.008	0.916	1.302	-0.447	1.494	46.54	1.07	1.884	-0.041	0.231	0.339	0.842	0.2	0.844	
<i>G. truncatulinoides</i>	212	250	10	0.072	0.307	0.289	0.588	0.047	-0.834	1.028	-0.56	0.245	0.148	-0.691	0.048	-0.758	-1.398	0.574	0.371	-0.241	0.624	1.564	-0.33	1.467	1.889	-0.1	0.564	0.402	2.278			
<i>G. truncatulinoides</i>	212	250	11	0.309	0.176	0.73	-0.053	1.186	0.088	0.975	0.962	1.930	1.269	0.881	0.395	0.056	0.179	0.198	1.697	1.387	0.652	0.396	0.773	1.073	0.652	0.396	0.773	1.073	0.652	0.396		
<i>G. truncatulinoides</i>	212	250	12	0.328	0.31	0.437	0.447	0.787	0.67	0.856	0.391	0.637	-0.636	0.132	-0.822	-0.732	0.993	0.611	0.164	0.624	1.564	0.33	1.467	1.889	-0.1	0.564	0.402	2.278				
<i>G. truncatulinoides</i>	212	250	13	-0.03	-0.475	0.012	0.901	0.263	-0.187	1.153	-1.02	0.535	1.449	-0.812	0.78	-0.403	-0.696	0.355	0.099	-0.326	1.475	0.601	1.072	0.07	1.662	-0.03	0.339	1.331	1.61	-0.841		
<i>G. truncatulinoides</i>	212	250	14	0.428	0.838	1.201	0.139	0.435	0.451	0.162	0.984	0.599	1.212	-0.23	2.451	1.041	0.467	0.291	1.238	1.502	0.279	1.231	0.889	0.481	0.981	0.219	1.547	0.808				
<i>G. truncatulinoides</i>	212	250	15	1.282	-0.495	0.470	-0.309	0.132	-0.387	0.1939	-0.454	0.126	0.117	1.12	1.187	-0.068	0.129	0.158	0.967	-0.327	0.97	1.894	-1.48	1.692	-0.04	0.233	0.331	0.739				
<i>G. truncatulinoides</i>	212	250	16	-0.104	-0.032	0.108	0.167	0.732	1.168	1.047	0.732																					

## Size-isotopic relationship in planktonic foraminifera

Shaded columns represent samples that were determined to be not normally distributed:  
Outliers were removed from this dataset

Species	Size	Specimen no.	Depth in core (cm)																										
			729	732	736	744	748	752	756	760	764	768	772	776	780	784	788	792	804	808	812	816	820	824	828				
G. bulloides	212	250	1	-0.874	-0.405	-0.559	-1.441	-1.014	-1.469	-0.586	-0.787	0.14	-1.183	-0.499	-0.186	-0.619	-0.417	-1.355	-0.396	-1.956	-0.300	-0.299	0.095	-0.161	-0.384	-1.597	-1.037	-1.137	-1.415
G. bulloides	212	250	2	-0.831	-0.721	-1.155	-1.804	-1.373	-0.589	-1.407	-1.220	-0.765	-1.274	-1.290	-1.363	-0.754	-1.329	-0.898	-2.002	-2.466	-1.081	-0.898	-1.241	-0.789	-1.010	-2.200	-0.812	-1.020	-0.812
G. bulloides	212	250	3	-0.003	-0.735	-0.015	-0.749	-0.728	-0.843	-1.085	-0.666	-1.956	-0.607	-0.851	-0.862	-1.803	-1.148	-0.610	-1.241	-0.789	-1.010	-0.289	-0.025	-0.010	-0.001	-0.001	-0.001	-0.001	-0.001
G. bulloides	212	250	4	-0.022	-0.340	-0.039	-0.415	-1.064	-0.963	-1.746	-0.078	-0.713	-0.125	-0.215	-0.411	-0.805	-0.094	-0.543	-0.863	-1.482	-1.002	-0.800	-0.404	-0.288	-0.100	-0.200	-0.184	-0.142	-0.142
G. bulloides	212	250	5	0.071	-0.496	-0.794	-0.446	-1.993	-0.655	-1.554	-0.542	-0.632	-0.831	-0.737	-1.591	-1.109	-1.079	-1.121	-0.856	-0.404	-0.288	-0.615	-1.005	-1.156	-1.209	-1.040	-0.283	-0.651	-1.854
G. bulloides	212	250	6	-0.775	-0.416	-0.841	-1.145	-1.096	-1.990	-0.895	-0.279	-0.305	-1.281	-0.107	-0.302	-2.190	-0.802	-0.334	-1.302	-0.025	-0.010	-0.001	-0.001	-0.001	-0.001	-0.001	-0.001	-0.001	-0.001
G. bulloides	212	250	7	-0.498	-0.760	-1.291	-1.401	-0.330	-1.159	-0.920	-0.670	-0.020	-0.129	-0.460	-0.338	-0.882	-1.596	-1.764	-1.081	-0.548	-0.106	-0.152	-0.173	-0.769	-0.553	-0.877	-1.528	-0.263	-1.799
G. bulloides	212	250	8	-0.982	-0.633	-1.496	-0.287	-0.800	-0.950	-0.932	-0.800	-0.728	-1.394	-0.799	-0.880	-0.446	-1.269	-1.432	-0.376	-1.751	-0.593	-0.232	-0.025	-0.001	-0.001	-0.001	-0.001	-0.001	-0.001
G. bulloides	212	250	9	-0.749	-1.038	-1.798	-0.363	-0.443	-1.390	-0.732	-0.597	-0.796	-0.840	-0.658	-0.549	-0.380	-0.691	-1.143	-0.928	-1.570	-0.107	-0.681	-1.229	-0.669	-1.746	-1.763	-1.614	-1.013	-1.471
G. bulloides	212	250	10	-0.072	-0.908	-1.596	-0.790	-1.089	-0.641	-0.708	-0.560	-0.462	-0.248	-0.703	-0.313	-1.429	-1.481	-1.272	-0.267	-0.698	-1.081	-1.205	-0.895	-1.130	-0.839	-1.105	-1.022	-0.812	-1.022
G. bulloides	212	250	11	-0.307	-0.555	-0.072	-0.101	-0.319	-1.165	-0.499	-1.056	-0.400	-0.074	-1.438	-1.024	-1.304	-0.783	-1.285	-1.758	-0.303	-0.520	-0.280	-0.025	-0.001	-0.001	-0.001	-0.001	-0.001	-0.001
G. bulloides	212	250	12	-0.811	-0.281	-1.225	-0.991	-2.254	-0.001	-0.781	-0.258	-0.407	-0.736	-0.203	-1.400	-1.202	-1.177	-0.779	-1.066	-0.430	-0.280	-0.802	-0.877	-1.627	-1.703	-1.021	-1.846	-1.499	-1.021
G. bulloides	212	250	13	-0.919	-0.236	-0.525	-0.384	-0.317	-1.556	-1.240	-0.575	-0.573	-0.522	-1.133	-1.215	-1.519	-1.826	-1.639	-1.708	-0.204	-0.332	-0.025	-0.001	-0.001	-0.001	-0.001	-0.001	-0.001	-0.001
G. bulloides	212	250	14	-0.520	-0.083	-1.365	-1.154	-1.310	-1.167	-0.284	-0.791	-0.154	-1.060	-0.971	-2.523	-0.867	-0.721	-0.815	-0.625	-1.626	-0.118	-0.474	-1.926	-0.977	-0.023	-0.023	-0.023	-0.023	-0.023
G. bulloides	212	250	15	-0.887	-0.283	-1.154	-1.607	-0.690	-0.151	-0.066	-0.421	-1.144	-1.064	-0.769	-0.994	-0.250	-0.880	-0.204	-0.774	-0.591	-0.563	-0.189	-0.189	-0.189	-0.189	-0.189	-0.189	-0.189	-0.189
G. bulloides	212	250	16	-0.487	-0.387	-0.992	-1.626	-0.221	-0.827	-0.728	-0.139	-0.305	-1.681	-1.187	-1.544	-0.825	-0.907	-1.500	-0.406	-0.364	-0.971	-1.376	-1.261	-1.743	-1.889	-1.316	-1.047	-1.047	-1.047
G. bulloides	212	250	17	-0.061	0.187	-1.762	-1.008	-0.153	-0.751	-1.348	-0.320	-0.533	-1.646	-1.383	-1.047	-1.155	-0.425	-0.008	-0.028	-0.015	-0.442	-0.507	-1.086	-0.814	-1.467	-1.467	-1.467	-1.467	-1.467
G. bulloides	212	250	18	-0.016	-0.423	-1.058	-0.784	-0.762	-1.008	-0.222	-0.059	-0.547	-0.812	-0.764	-0.631	-1.715	-0.479	-0.547	-0.783	-0.578	-0.232	-0.025	-0.001	-0.001	-0.001	-0.001	-0.001	-0.001	-0.001
G. bulloides	212	250	19	-0.017	-0.097	-1.058	-0.784	-1.058	-0.784	-0.619	-1.010	-1.463	-1.687	-1.472	-1.008	-1.010	-0.831	-0.835	-2.809	-1.237	-1.158	-1.076	-1.076	-1.076	-1.076	-1.076	-1.076	-1.076	-1.076
G. bulloides	212	250	20	-0.030	-0.030	-1.702	-1.023	-0.253	-0.895	-0.697	-0.038	-0.705	-1.591	-1.097	-0.841	-0.801	-0.746	-0.063	-0.380	-0.460	-0.283	-0.025	-0.001	-0.001	-0.001	-0.001	-0.001	-0.001	-0.001
G. bulloides	250	300	1	-0.438	-0.694	-0.484	-0.393	-0.811	-0.961	-1.164	-0.148	-0.889	-1.189	-0.954	-0.636	-0.697	-0.038	-0.705	-1.591	-1.097	-0.841	-0.801	-0.746	-0.063	-0.380	-0.460	-0.283	-1.546	-1.546
G. bulloides	250	300	2	-0.028	-0.156	-1.385	-0.853	-0.974	-1.746	-0.443	-0.361	-0.754	-1.047	-0.329	-0.211	-0.373	-0.120	-0.712	-0.515	-1.155	-0.96	-0.96	-0.96	-0.96	-0.96	-0.96	-0.96	-0.96	-0.96
G. bulloides	250	300	3	-0.153	-0.441	-0.656	-1.522	-2.380	-0.491	-1.456	-1.249	-0.851	-0.986	-0.909	-0.979	-0.756	-0.278	-0.005	-1.311	-0.791	-1.740	-0.680	-0.906	-1.104	-0.968	-0.804	-0.314	-1.177	
G. bulloides	250	300	4	-0.172	-0.470	-1.200	-1.191	-1.634	-0.643	-1.736	-0.778	-0.660	-0.423	-0.241	-0.722	-0.808	-0.556	-0.513	-0.919	-0.374	-0.447	-0.001	-0.001	-0.001	-0.001	-0.001	-0.001	-0.001	-0.001
G. bulloides	250	300	5	-0.314	-0.623	-1.169	-0.689	-0.004	-1.218	-0.897	-1.338	-1.249	-0.052	-0.116	-0.645	-1.001	-0.475	-0.948	-1.240	-0.510	-1.246	-0.495	-1.194	-0.623	-0.808	-0.728	-0.821	-1.131	-1.545
G. bulloides	250	300	6	-0.428	-0.509	-1.118	-1.210	-0.303	-1.033	-1.262	-0.493	-0.748	-0.891	-0.660	-0.203	-1.006	-0.356	-1.063	-0.771	-0.959	-0.678	-0.712	-0.872	-1.110	-1.009	-0.951	-1.186	-1.011	-1.011
G. bulloides	250	300	7	-0.754	-1.391	-1.087	-0.718	-1.429	-1.628	-1.144	-1.042	-0.295	-0.397	-0.820	-0.734	-0.308	-1.007	-1.093	-1.282	-1.240	-1.890	-0.025	-0.010	-0.001	-0.001	-0.001	-0.001	-0.001	-0.001
G. bulloides	250	300	8	-0.855	-0.361	-1.615	-1.121	-0.762	-0.869	-1.431	-0.245	-0.748	-0.464	-0.558	-0.431	-1.660	-0.241	-1.181	-1.660	-0.241	-1.181	-0.241	-1.181	-0.241	-1.181	-0.241	-1.181	-0.241	-1.181
G. bulloides	250	300	9	-2.05	-0.619	-0.439	-1.168	-0.302	-1.192	-1.078	-1.316	-0.644	-0.791	-0.511	-0.316	-0.449	-1.182	-0.748	-0.925	-1.028	-1.108	-0.025	-0.010	-0.001	-0.001	-0.001	-0.001	-0.001	-0.001
G. bulloides	250	300	10	-1.017	-0.897	-1.081	-0.639	-0.443	-1.039	-1.039	-1.039	-1.039	-1.039	-1.039	-1.039	-1.039	-1.039	-1.039	-1.039	-1.039	-1.039	-1.039	-1.039	-1.039	-1.039	-1.039	-1.039	-1.039	-1.039
G. bulloides	250	300	11	-0.272	-0.065	-1.104	-0.835	-0.208	-0.960	-0.529	-1.034	-0.768	-0.464	-0.069	-0.319	-0.366	-1.044	-1.280	-0.980	-0.855	-1.832	-0.025	-0.010	-0.001	-0.001	-0.001	-0.001	-0.001	-0.001
G. bulloides	250	300	12	-0.561	-0.512	-1.035	-0.687	-0.277	-2.251	-0.055	-0.944	-1.731	-1.931	-0.421	-0.851	-1.064	-1.214	-1.370	-0.613	-1.050	-1.389	-1.036	-0.710	-0.302	-1.400	-1.229	-1.646	-0.505	-0.466
G. bulloides	250	300	13	-0.223	-0.591	-0.882	-0.085	-0.743	-1.177	-0.173	-0.272	-0.478	-0.278	-0.208	-0.376	-0.134	-0.587	-1.001	-0.991	-0.263	-0.817	-0.674	-0.674	-0.674	-0.674	-0.674	-0.674	-0.674	-0.674
G. bulloides	250	300	14	-0.690	-1.310	-1.317	-0.810	-0.766	-1.495	-1.044	-0.650	-0.580	-0.327	-0.179	-0.334	-0.986	-1.324	-1.145	-1.534	-0.824	-0.999	-0.474	-0.474	-0.474	-0.474	-0.474	-0.474	-0.474	-0.474
G. bulloides	250	300	15	-0.289	-0.990	-0.647	-0.055	-0.411	-0.839	-0.977	-1.039	-0.645	-0.419	-0.829	-0.977	-1.039	-0.645	-0.419	-0.829	-0.977	-1.039	-0.645	-0.419	-0.829	-0.977	-1.039	-0.645	-0.419	-0.829
G. bulloides	250	300	16	-0.218	-0.426	-0.248	-1.168	-1.731	-1.703	-0.699	-0.590	-0.552	-0.741	-0.251	-0.869	-1.044	-0.919	-1.301	-1.082	-0.467	-0.467	-0.467	-0.467	-0.467	-0.467	-0.467	-0.467	-0.467	-0.467
G. bulloides	250	300	17	-0.416	-0.135	-1.025	-0.507	-1.020	-1.424	-1.106	-0.165	-0.289	-0.150	-0.365	-0.332	-0.888	-0.384	-0.651	-1.107	-1.023	-0.731	-0.792	-0.099	-0.266	-0.308	-1.644	-1.862	-1.258	-1.080
G. bulloides	250	300	18	-0.083	-0.444	-0.363	-1.501	-0.743	-1.163	-0.429	-0.744	-0.88																	





sample t-test was performed on the differences, smallest size fraction value minus the largest, between the means of the size fractions of both  $\delta^{18}\text{O}$  (Table 8.3) and  $\delta^{13}\text{C}$  (Table 8.5). This statistical choice is the result of speed and efficiency as it would require six paired t-tests per sample multiplied by 26 samples, increasing the likelihood of an error associated with a false positive. The null hypothesis of the performed test is that the difference in  $\delta^{18}\text{O}$  and  $\delta^{13}\text{C}$  between two size fractions is zero ( $H_0: \mu_1 - \mu_2 = 0$ ), thus all means are equal ( $H_0: \mu_1 = \mu_2 = \mu_3 = \mu_4$ ), and the resultant hypothesis is that at least one of the means is different from the others are different ( $H_1: \mu_1 \neq \mu_2 \neq \mu_3 \neq \mu_4$ ). Analysis was performed at both the 90% and 95% confidence level ( $\alpha$  values of 0.10 and 0.05; critical t-values of 2.015 and 2.571 respectively). For (2) testing whether the relationship remains constant through time over a large climatic perturbation a two tailed t-test for dependent samples was performed between size fractions for the entire core ( $n = 6$ ). The  $H_0$  is that the differences between size fractions is zero, thus all means are equal and that this is consistent down core. The critical values of the t distribution for  $n = 26$  samples of the 90% and 95% confidence level ( $\alpha$  values of 0.10 and 0.05) are 1.708 and 2.060 respectively. No ice volume correction prior to statistical analysis was performed as it was deemed that the difference between two size fractions within the same sample should negate this effect.

The down core means of the smallest (212-250  $\mu\text{m}$ ) and largest (355-400  $\mu\text{m}$ ) specimens of all species were plotted against each other for both  $\delta^{18}\text{O}$  and  $\delta^{13}\text{C}$  respectively as per *Sarkar et al.* [1990] (Table 8.4). The resultant slope was tested against a 1:1 relationship or iso- $\delta$  line using a two-tailed t-test, the slope of such a line is considered to be unity as  $y$  would be equal to  $x$  ( $H_0$ : slope = 1;  $H_1$ : slope  $\neq$  1). Deviations from the iso- $\delta$  line would indicate a change in the relative depletion or enrichment between the two size fractions at either the warm or cold temperature end for  $\delta^{18}\text{O}$ . To calculate the estimated standard error of the regression the vertical difference between the observed and fitted values, using a linear regression, was calculated using an ordinary least squares (OLS), which minimizes the resultant sum of the squared residuals (SSR). The magnitude of the SSR is influenced by the number of data points, a larger number of datapoints

Test values for smallest-largest crossplot					
Species	y = ax+b		r <sup>2</sup>	T test value for r <sup>2</sup> †	T value‡
	a	b			
<b>Oxygen isotope values</b>					
<i>G. bulloides</i>	0.8033	0.4535	0.6432	6.5776	-1.305
<i>G. inflata</i>	0.5687	1.5919	0.3433	3.5421	-1.288
<i>G. truncatulinoides</i>	0.8929	1.8467	0.6626	6.853	-1.669
<b>Carbon isotope values</b>					
<i>G. bulloides</i>	0.2345	-0.324	0.1315	1.9063	-2.319
<i>G. inflata</i>	0.1277	0.6448	0.1107	1.7284	-3.393
<i>G. truncatulinoides</i>	0.2231	0.7924	0.0775	1.42	-2.887

†Where,  $H_0: p = 0$ ,  $H_1: p \neq 0$ . Two tailed t-test value for  $\alpha$  0.05 is 2.064

‡Where,  $H_0$ : slope = 1,  $H_1: p \neq 1$ . Two tailed t-test value for  $\alpha$  0.05 is 2.064

Table 8.4. Smallest and largest size fraction linear regression and t-test values.



1

2

3

4

5

6

7

8

9

[illegible]



results in a larger SSR, to account for this it was divided by the degrees of freedom (n-2). The resultant expression was square rooted. The test value at  $\alpha$  0.05 for two tailed is 2.064 for n = 26.

Interdependence, or the degree of linear relationship, between  $\delta^{18}\text{O}$  and  $\delta^{13}\text{C}$  was tested for using covariance upon the outlier corrected values of oxygen and carbon for each size fraction and for all size fractions combined (Table 8.6 and 8.7) using the PAST software package [Hammer *et al.*, 2001]. Independence, where  $\delta^{18}\text{O}$  and  $\delta^{13}\text{C}$  vary without a connection, is implied when covariance has a value of 0, or the relationship between the two parameters is nonlinear. The

Table 8.6. Covariance of studied planktonic foraminifera. Test values for covariance and correlation coefficient of *G. bulloides*.

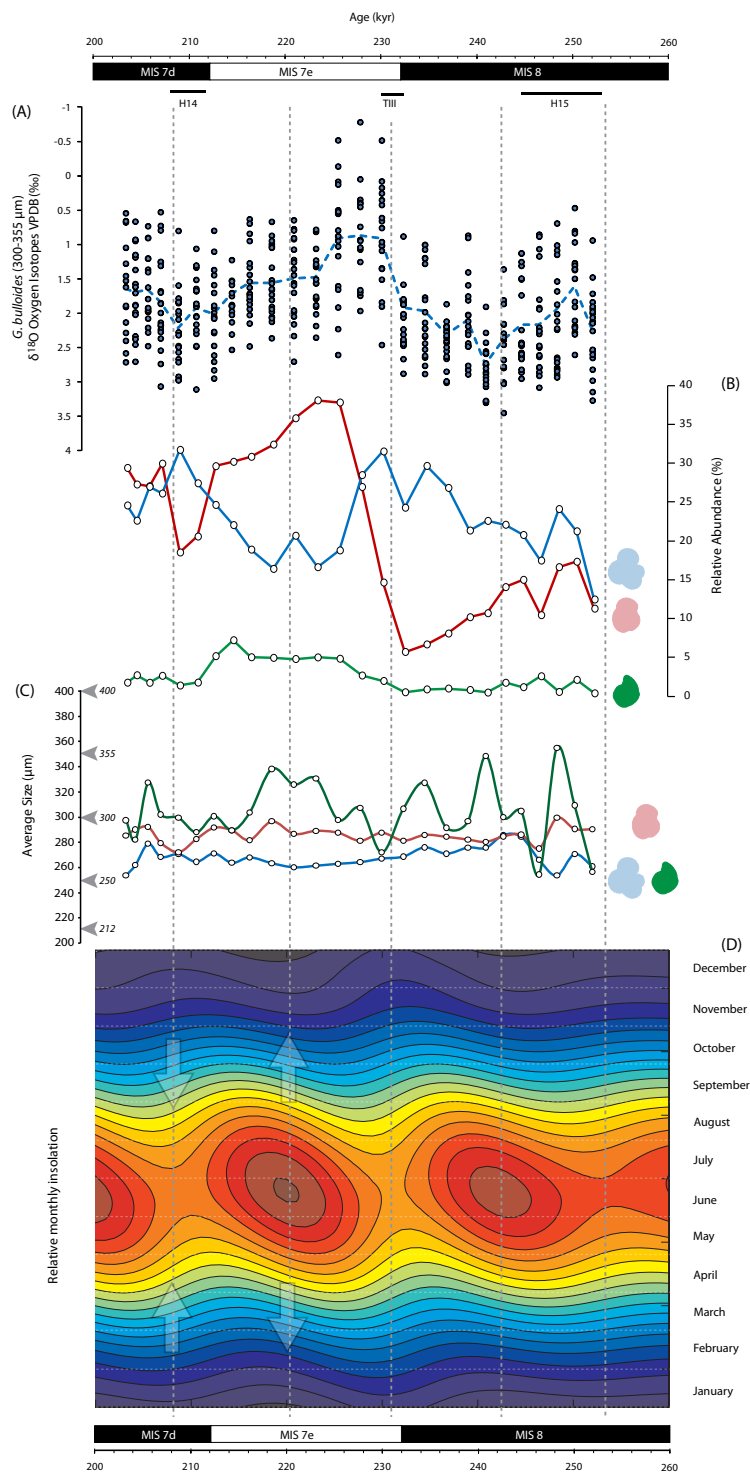
Depth in Core (cm)	Age (ky)	G. bulloides										Combined										
		Covariance					Product of Standard Deviations					Correlation Coefficient		Color	StDev. P.	Corr. Coef.						
		212-250 $\mu\text{m}$	250-300 $\mu\text{m}$	300-365 $\mu\text{m}$	365-400 $\mu\text{m}$	212-250 $\mu\text{m}$	250-300 $\mu\text{m}$	300-365 $\mu\text{m}$	365-400 $\mu\text{m}$	212-250 $\mu\text{m}$	250-300 $\mu\text{m}$	300-365 $\mu\text{m}$	365-400 $\mu\text{m}$									
729	203.4	0.00	-0.02	0.07	0.19	0.20	0.26	0.27	0.30	0.01	-0.06	0.24	0.65	0.08	0.29	0.28						
732	204.4	-0.04	0.01	0.06	0.09	0.19	0.39	0.19	0.36	-0.21	0.02	0.33	0.26	0.03	0.30	0.10						
736	205.7	-0.02	0.13	0.20	0.05	0.52	0.62	0.28	0.21	-0.03	0.26	0.72	0.41	0.11	0.43	0.24						
740	207.0	0.46	0.16	0.16	0.15	0.72	0.39	0.29	0.33	0.67	0.41	0.55	0.45	0.34	0.55	0.61						
744	208.9	0.23	-0.04	-0.09	0.22	0.57	0.40	0.24	0.41	-0.11	-0.37	0.52	0.14	0.58	0.58	0.25						
748	210.7	0.17	0.24	0.07	-0.04	0.64	0.48	0.23	0.18	0.27	0.50	0.30	-0.20	0.05	0.44	0.12						
752	212.6	-0.03	0.11	0.07	0.13	0.26	0.32	0.29	0.33	-0.12	0.35	0.26	0.40	0.06	0.39	0.16						
756	214.5	0.00	0.20	0.12	0.07	0.19	0.38	0.21	0.27	0.00	0.53	0.57	0.27	0.09	0.31	0.28						
760	216.3	0.32	0.08	0.04	0.00	0.56	0.25	0.17	0.22	0.56	0.34	0.22	-0.01	0.09	0.33	0.28						
764	218.6	0.22	0.09	0.11	0.20	0.31	0.31	0.22	0.32	0.71	0.28	0.48	0.64	0.17	0.32	0.52						
768	220.9	0.25	0.11	-0.01	0.07	0.34	0.24	0.22	0.19	0.75	0.45	-0.03	0.35	0.12	0.30	0.40						
772	223.2	0.37	0.08	0.02	0.12	0.63	0.29	0.24	0.18	0.58	0.27	0.09	0.65	0.14	0.37	0.39						
776	225.5	0.34	0.20	0.05	0.11	0.59	0.39	0.34	0.21	0.58	0.51	0.16	0.51	0.14	0.42	0.34						
780	227.8	0.14	0.07	-0.03	0.02	0.33	0.40	0.29	0.21	0.44	0.17	-0.12	0.08	0.08	0.34	0.22						
784	230.1	0.24	0.07	0.02	0.09	0.52	0.29	0.33	0.29	0.47	0.24	0.05	0.32	0.16	0.44	0.38						
788	232.3	0.08	0.14	0.01	0.02	0.24	0.42	0.34	0.33	0.32	0.34	0.04	0.07	0.07	0.34	0.21						
792	234.6	0.52	-0.06	-0.04	0.04	0.66	0.28	0.20	0.16	0.79	-0.23	-0.20	0.26	0.12	0.35	0.34						
796	236.8	0.42	0.17	0.01	0.02	0.66	0.41	0.19	0.26	0.64	0.42	0.03	0.09	0.15	0.39	0.37						
800	239.1	0.15	0.38	0.04	0.06	0.40	0.46	0.28	0.12	0.38	0.83	0.13	0.48	0.15	0.33	0.47						
804	240.9	0.27	0.13	0.00	0.09	0.53	0.33	0.13	0.15	0.51	0.38	0.01	0.58	0.14	0.33	0.43						
808	242.8	0.10	0.22	0.07	0.01	0.35	0.31	0.25	0.27	0.27	0.71	0.27	0.03	0.11	0.36	0.31						
812	244.6	0.07	0.15	-0.06	0.07	0.41	0.24	0.35	0.24	0.16	0.64	-0.17	0.28	0.22	0.47	0.46						
816	246.5	0.13	0.05	0.16	0.04	0.38	0.20	0.29	0.22	0.35	0.26	0.53	0.17	0.15	0.38	0.40						
820	248.4	0.00	0.10	0.08	0.06	0.57	0.47	0.44	0.26	0.01	0.22	0.19	0.24	0.10	0.49	0.20						
824	250.2	0.09	-0.06	0.01	-0.02	0.41	0.31	0.26	0.18	0.23	-0.19	0.03	-0.10	0.01	0.29	0.05						
828	252.1	-0.08	-0.05	0.07	0.01	0.39	0.28	0.25	0.11	-0.20	-0.20	0.30	0.12	-0.01	0.26	-0.02						
Average		0.33					0.28					0.18					0.29		Average		0.30	

Depth in Core (cm)	Age (kyr)	G. inflata												Combined StDev. Pr.		Corr. Coef.	
		Covariance				Product of Standard Deviations				Correlation Coefficient							
		212-250 $\mu\text{m}$	250-300 $\mu\text{m}$	300-355 $\mu\text{m}$	355-400 $\mu\text{m}$	212-250 $\mu\text{m}$	250-300 $\mu\text{m}$	300-355 $\mu\text{m}$	355-400 $\mu\text{m}$	212-250 $\mu\text{m}$	250-300 $\mu\text{m}$	300-355 $\mu\text{m}$	355-400 $\mu\text{m}$	Co/var	Average		
729	203.4	0.18	0.04	0.00	0.01	0.26	0.08	0.14	0.05	0.67	0.47	0.01	0.24	0.17	0.24	0.69	
732	204.4	0.13	0.04	-0.02	0.01	0.26	0.16	0.09	0.11	0.51	0.22	-0.18	0.55	0.29	0.33	0.74	
736	205.7	0.25	0.07	0.01	0.06	0.30	0.13	0.07	0.08	0.84	0.52	0.17	0.70	0.26	0.39	0.81	
740	207.0	0.15	0.02	0.06	0.00	0.25	0.11	0.10	0.08	0.60	0.15	0.56	-0.04	0.14	0.24	0.60	
744	208.9	0.18	0.07	0.00	0.03	0.27	0.16	0.14	0.09	0.67	0.43	-0.03	0.32	0.34	0.44	0.76	
748	210.7	0.28	0.10	0.07	0.01	0.38	0.29	0.19	0.07	0.73	0.34	0.36	0.10	0.16	0.28	0.56	
752	212.6	0.23	0.05	0.02	0.04	0.34	0.13	0.08	0.09	0.67	0.42	0.20	0.43	0.42	0.84	0.84	
756	214.5	0.18	0.02	0.01	0.11	0.27	0.10	0.08	0.18	0.68	0.20	0.17	0.60	0.46	0.54	0.84	
760	216.3	0.24	0.47	0.02	0.05	0.35	0.60	0.07	0.16	0.69	0.79	0.21	0.30	0.40	0.56	0.71	
764	218.6	0.44	0.28	0.02	0.07	0.51	0.52	0.15	0.10	0.87	0.55	0.11	0.70	0.49	0.61	0.80	
768	220.9	0.17	0.03	0.01	0.03	0.24	0.09	0.12	0.09	0.71	0.29	0.07	0.36	0.30	0.40	0.75	
772	223.2	0.21	0.04	0.06	0.02	0.25	0.14	0.10	0.08	0.83	0.30	0.57	0.26	0.20	0.29	0.68	
776	225.5	0.16	0.05	0.05	0.09	0.24	0.16	0.12	0.16	0.65	0.29	0.45	0.57	0.28	0.39	0.73	
780	227.8	0.08	0.04	0.07	0.01	0.13	0.12	0.18	0.08	0.59	0.31	0.39	0.08	0.36	0.46	0.78	
784	230.1	0.11	0.02	0.02	0.03	0.20	0.11	0.08	0.12	0.54	0.16	0.20	0.28	0.23	0.34	0.69	
788	232.3	0.37	0.01	0.09	0.06	0.55	0.17	0.26	0.27	0.67	0.03	0.33	0.23	0.41	0.57	0.72	
792	234.6	0.10	0.08	0.05	-0.01	0.19	0.29	0.19	0.11	0.56	0.28	0.28	-0.12	0.21	0.36	0.58	
796	236.8	0.24	0.11	0.00	0.05	0.36	0.56	0.11	0.12	0.67	0.20	-0.01	0.42	0.20	0.51	0.39	
800	239.1	0.23	0.40	0.02	0.11	0.55	0.54	0.19	0.14	0.42	0.75	0.08	0.78	0.39	0.61	0.64	
804	240.9	0.34	0.03	0.01	0.10	0.52	0.21	0.18	0.24	0.66	0.12	0.06	0.42	0.42	0.60	0.70	
808	242.8	0.39	0.16	-0.02	0.03	0.45	0.26	0.12	0.10	0.86	0.62	-0.17	0.30	0.45	0.58	0.78	
812	244.6	0.35	0.20	0.14	0.01	0.46	0.29	0.23	0.10	0.75	0.70	0.60	0.09	0.60	0.72	0.82	
816	246.5	0.27	0.02	0.01	-0.03	0.54	0.19	0.11	0.13	0.51	0.08	0.05	-0.23	0.15	0.33	0.45	
820	248.4	0.37	0.04	0.00	0.08	0.48	0.24	0.09	0.21	0.77	0.15	-0.02	0.37	0.29	0.43	0.68	
824	250.2	0.07	0.04	0.03	0.03	0.15	0.17	0.18	0.13	0.45	0.25	0.17	0.25	0.30	0.41	0.72	
828	252.1	0.01	0.02	0.08	0.10	0.27	0.27	0.21	0.18	0.04	0.07	0.39	0.54	0.11	0.35	0.30	
		Average				Average				Average				Average		Average	
														0.64		0.33	
														0.33		0.19	
														0.33		0.68	

Table 8.7. Covariance of studied planktonic foraminifera. Test values for covariance and correlation coefficient of *G. inflata*.

degree to which values larger than 0 are independent necessitates transformation into a dimensionless quantity independent of scaling relationships. Therefore we interpret the data using the correlation coefficient, in which the covariance is divided by the product of the standard deviation of both oxygen and carbon. Such transformation gives a limit of  $\pm 1$ , in which values that approach  $\pm 1$  represent a higher degree of linear co-dependence.





### 8.3 Results

#### 8.3.1 Faunal abundance counts and Size

*Globorotalia truncatulinoides* (<10%) and *G. inflata* (~10-40%) have higher abundance corresponding with the warmer interval of MIS7e and lower abundance during the preceding cold interval (MIS8) (Figure 8.3). The abundance of *G. bulloides* (~10-35%) appears to follow the expansion and contraction of insolation, with periods of reduced seasonality, *i.e.* milder (lower insolation) summer and winter months, showing higher relative abundances (Figure 8.3). Calculated average size for this interval falls between 250-300  $\mu\text{m}$  for both *G. bulloides* and *G. inflata* with only minor variation (~30  $\mu\text{m}$ ) (Figure 8.3c). The size of *G. truncatulinoides* is more erratic varying between 250  $\mu\text{m}$  and 355  $\mu\text{m}$ , especially between 227-252 kyr in which the abundance of this species is low.

#### 8.3.2 Oxygen stable isotope values ( $\delta^{18}\text{O}$ )

The oxygen isotope values of *G. bulloides* (n=1921) and *G. truncatulinoides* (n = 1933) show the characteristic pattern consistent with a transition between a glacial, with values enriched in  $\delta^{18}\text{O}$ , and interglacial, with depleted  $\delta^{18}\text{O}$  values. Visually there is an overlap between the oxygen isotope values of all size fractions of *G. bulloides* whereas this is only present in the larger size fractions of both *G. inflata* (n = 1855) and *G. truncatulinoides* (Figure 8.4 and 8.5). For the latter two species the smaller size fraction (212-250  $\mu\text{m}$ ) appears to be relatively more depleted than the larger size fractions (250-400  $\mu\text{m}$ ). Plotting the mean, per sample, smallest (212-250  $\mu\text{m}$ ) and largest (355-400  $\mu\text{m}$ ) size fraction  $\delta^{18}\text{O}$  against each other (Figure 8.6), shows that the slopes of *G. bulloides*, *G. inflata* and *G. truncatulinoides* are statistically significant from 0 (t-test values for correlation coefficient: 6.5776, 3.5421 and 6.8653 respectively with a two tailed test value of 2.064 at  $\alpha$  0.05,  $H_0$ :  $p = 0$ ). However there is insufficient evidence to suggest that the value of the slope is statistically different from a 1:1 iso- $\delta$  line (t-test values for difference: -1.305, -1.288 and -1.669 respectively). At the minimum value the offset between smallest and largest size fractions is 0.45, 1.59 and 1.85 ‰, however given that the slopes are 0.80, 0.57 and 0.89 ‰ this value decreases with more enriched values, *i.e.* at colder values (Figure 8.6).

Figure 8.3. (opposite page) Size of planktonic foraminifera. For reference (a) *G. bulloides* single specimen  $\delta^{18}\text{O}$  values, dashed line represent average  $\delta^{18}\text{O}$  values. (b) Relative abundance of *G. bulloides* (blue), *G. inflata* (red) and *G. truncatulinoides* (green) used to calculate (c) the average size, arrows in (c) denote the upper and lower limits of the size fractions used in this study. In comparison with abundance and average size (d) the relative monthly insolation for the time period has been plotted. Arrows in (d) represent expansion and contraction of increased Summer insolation.



R & A

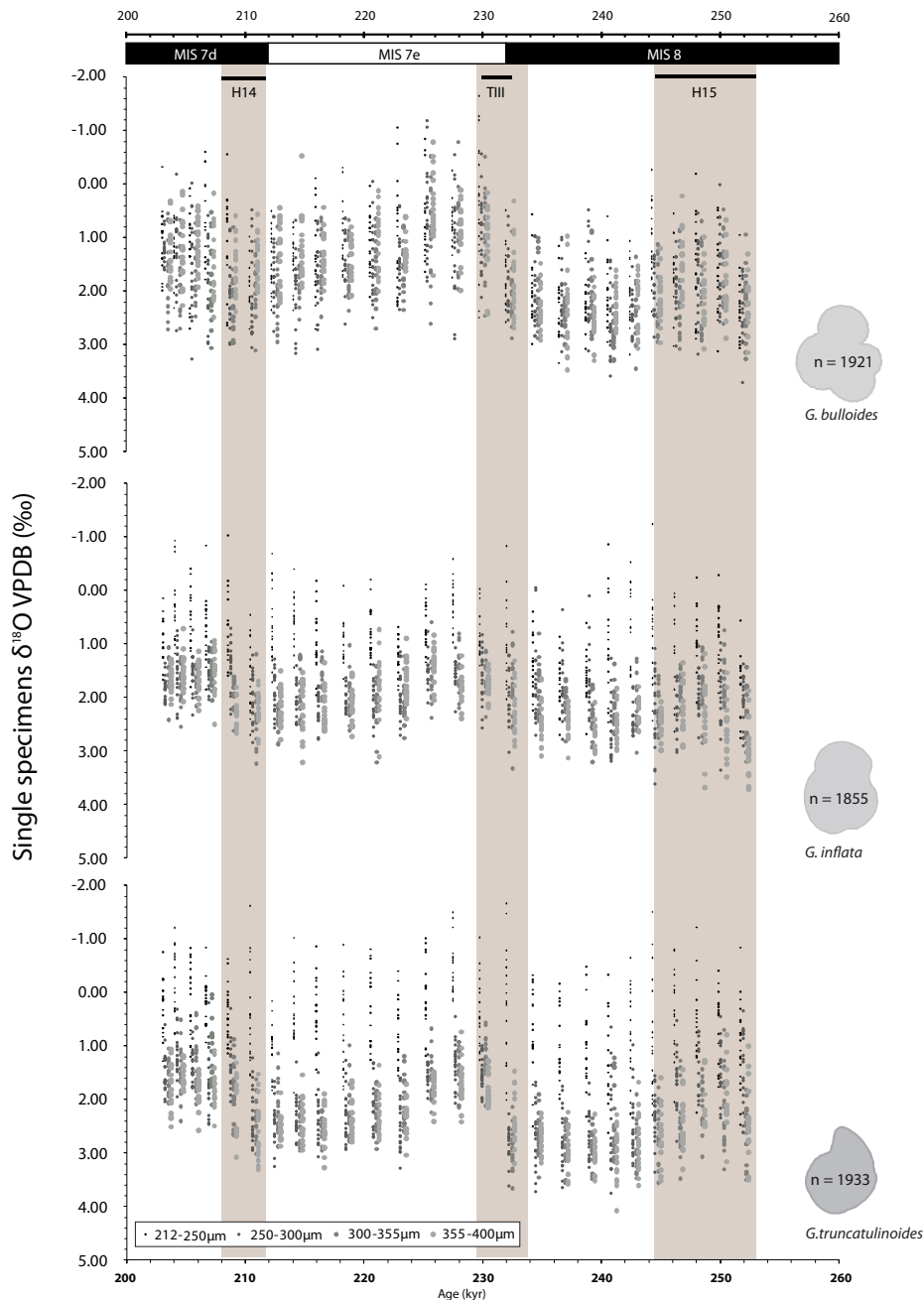


Figure 8.4. Single specimen oxygen isotope values. Raw  $\delta^{18}\text{O}$  values, the symbol size denotes size fraction, for convenience the data points are offset from one another. Shaded regions represent periods where ice rafted debris is present within the core, this envelope however is larger than the actual duration of a Heinrich event as it is difficult to constrain the precise date of such 'old' events.

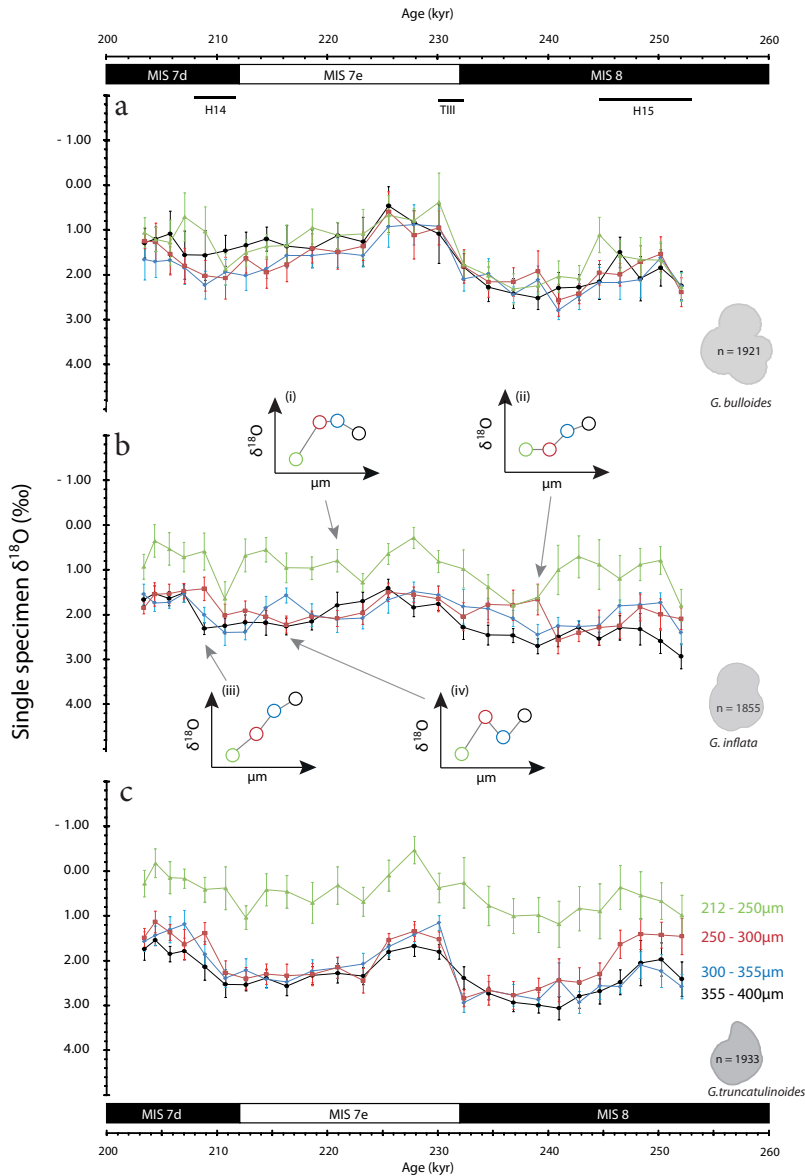


Figure 8.5. Mean oxygen isotope values with 95% confidence intervals. Mean  $\delta^{18}\text{O}$  values for (a) *G. bulloides*, (b) *G. inflata* and (c) *G. truncatulinoides*, colour denotes size fraction. Confidence intervals are based upon using the outlier corrected single specimen data to compute a t based confidence interval ( $n < 30$ ) at the 95% level ( $\alpha = 0.05$ ), assuming that the sample is normally distributed. Insets in (b) show the size versus oxygen isotope for (i) 220.9 kyr reminiscent of the study of *Ravelo and Fairbanks* [1992] (ii) 239.1 kyr, (iii) 208.9 kyr and (iv) 216.3 kyr. A one sample t-test shows that (i) and (iv) do not have sufficient evidence to reject the null hypothesis ( $H_0$ ) that the means are different, whereas (ii) and (iii) have sufficient evidence to accept the alternative hypothesis ( $H_1$ ).

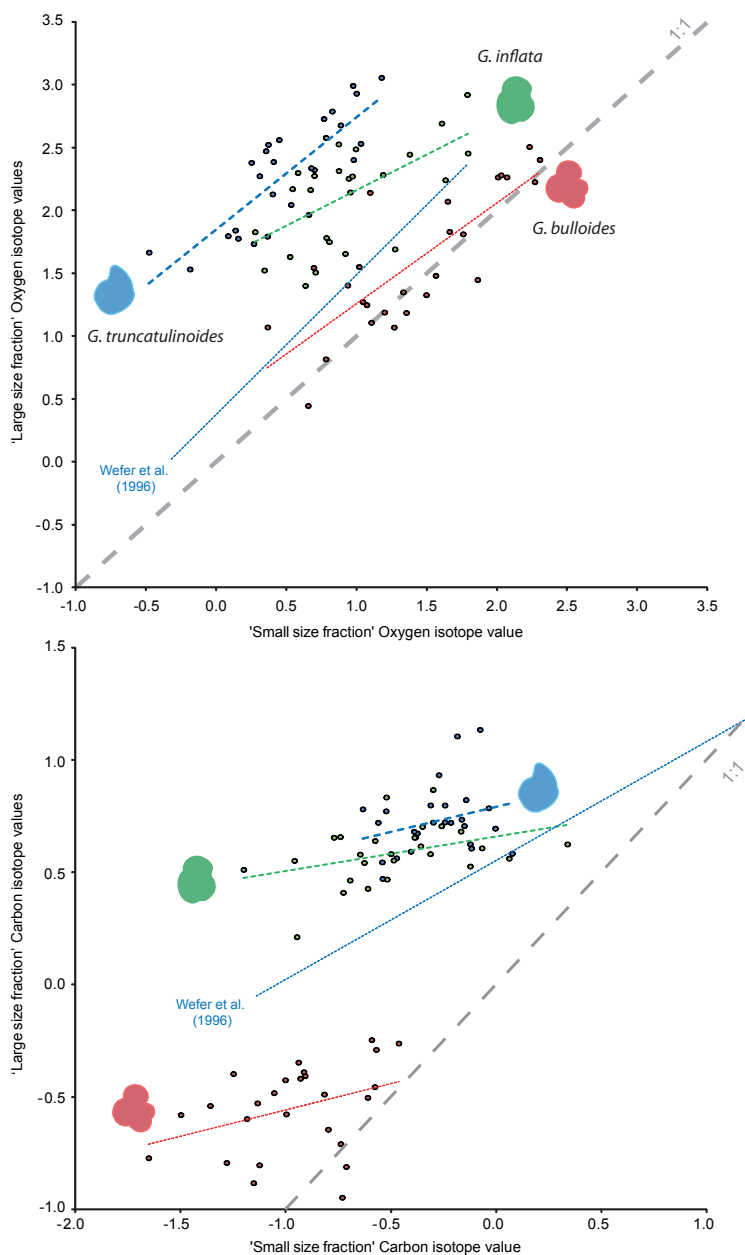


Figure 8.6. Isotope differences between smallest and largest size fraction. Isotope difference between the mean of the smallest (212–250  $\mu\text{m}$ ) and largest (355–400  $\mu\text{m}$ ) size fractions of (Top)  $\delta^{18}\text{O}$  and (Bottom)  $\delta^{13}\text{C}$ . The 1:1 ( $\delta$ -iso line) relationship (grey dashed line) is presented, equations of the linear regressions (coloured dashed lines), and resultant T-test values are presented in Table 8.4. The  $\delta$ -iso lines of *G. truncatulinoides* from Wefer et al. [1996] are presented for comparison.



For *G. bulloides* only 4 out of 26 samples show sufficient evidence to reject the null hypothesis thus for this species the size fractions have predominately the same mean values, whereas all size fractions show a statistical difference and thus the difference between size fractions is not constant (Table 8.3). For *G. inflata* 20 out of 26 samples show sufficient evidence to reject the null hypothesis thus for this species the size fractions have predominately different mean values, whereas apart from the difference between 250-300  $\mu\text{m}$  and 300-355  $\mu\text{m}$  all size fractions show a statistical difference and thus the difference between size fractions through time is not constant (Table 8.3). Whilst visually there appears to be a difference (Figure 8.5b), when viewed simply as the size-isotope relationship for a single sample then the statistical significance to either accept the alternative hypothesis (Figure 8.5b - i and iv) or reject the null hypothesis (Figure 8.5b- ii and iii) becomes apparent (See supplementary figures 1-6). For *G. truncatulinoides* 25 out of 26 samples show sufficient evidence to reject the null hypothesis, thus for this species the size fractions have predominately different mean  $\delta^{18}\text{O}$  values, whereas all size fractions show a statistical difference and thus the difference between size fractions is not constant (Table 8.3). Curiously the means of small specimens of *G. inflata* and *G. truncatulinoides* are more depleted and show differences from those of coeval small specimens of *G. bulloides*, this is not present in the other, larger, size fractions.

Comparison of the spread, using the standard deviation per size fraction (Supplementary Figure 8.7-8.8), in *G. bulloides* against the insolation difference between July and December reveals a negative correlation, with higher values of insolation difference associated with a lower standard deviation. The relationship is stronger ( $r = 0.5748$ ) however when the insolation difference between the months associated with the end of the deep Winter mixing and Summer stratification (March and June) in the modern ocean are used. It would appear that when the  $\Delta\delta^{18}\text{O}$  between small and large *G. inflata* ( $\Delta\delta^{18}\text{O}_{s-l}$ ) is reduced, so that the smallest specimens of *G. inflata* have similar values as larger specimens ( $>250\ \mu\text{m}$ ), insolation is halfway between a minimum and maximum, apart from at 234-239 kyr during the onset of the termination. During these transient events the  $\delta^{18}\text{O}$  of *G. inflata* shows a relationship with the  $\delta^{18}\text{O}$  of the largest size fraction (355-400  $\mu\text{m}$ ) of *G. bulloides* ( $r^2 = 0.4935$ ;  $n = 8$ ). Given that these events occur in relationship to the insolation the first derivative of the seasonal difference at  $45^\circ\text{N}$  was taken as the magnitude and direction of change in seasonality and compared with  $\Delta\delta^{18}\text{O}_{s-l}$  for *G. inflata*. This reveals that there is a linear relationship that positively correlates during MIS8 ( $r = 0.6538$ ) and negatively correlates during Interglacial MIS7 ( $r = 0.6882$ ).

### 8.3.3 Carbon stable isotope values ( $\delta^{13}\text{C}$ )

Carbon isotope values range between -2.00 ‰ and +1.50 ‰ (Figure's 7-8). The species range, between their maximum and minimum points for all samples, from the depleted values of -2.00 ‰ and 0.00 ‰ for *G. bulloides*, a range of -1.50 and +1.20 ‰ for *G. inflata* and enriched values of -1.00 to +1.50 ‰ for



R & A

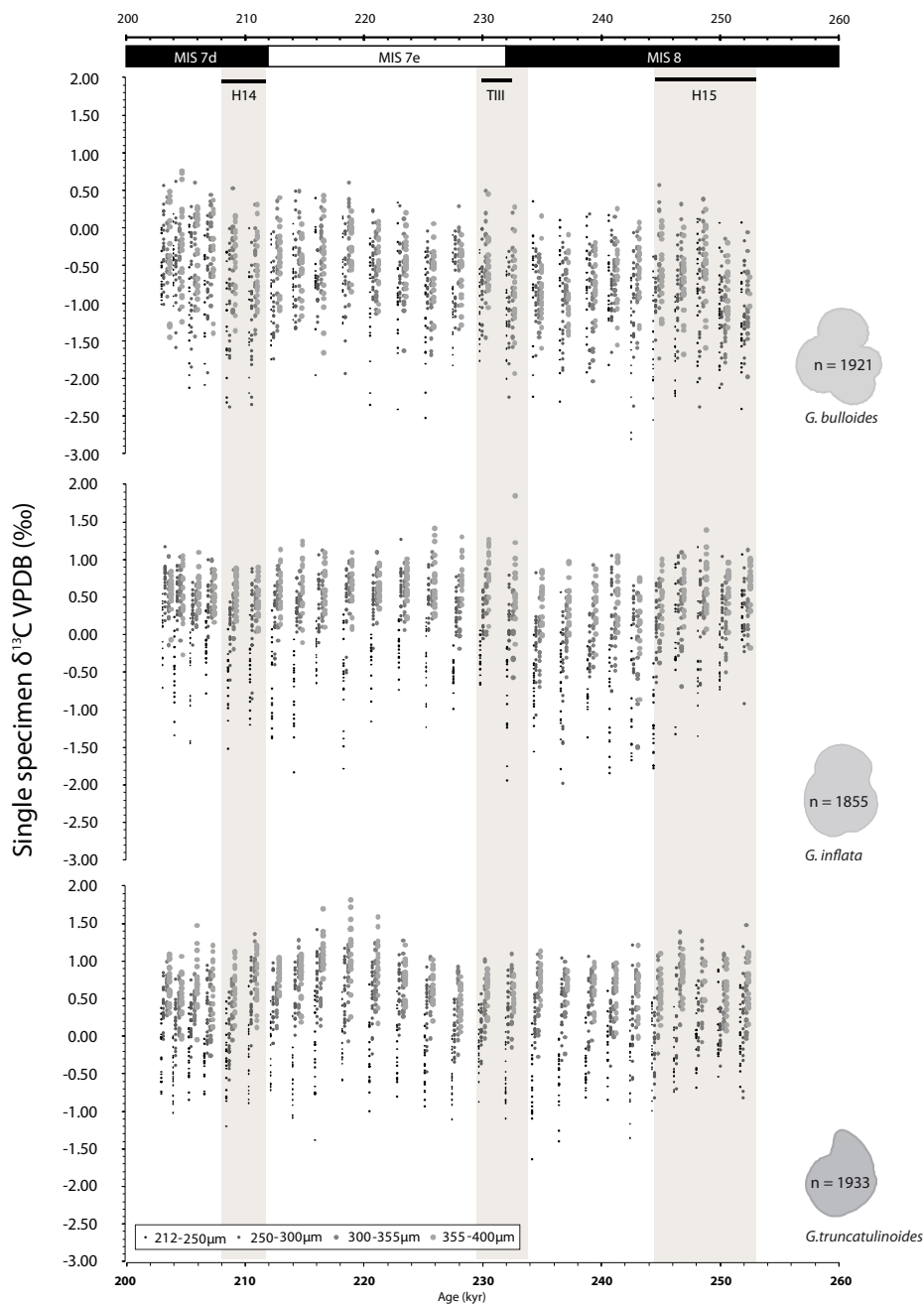


Figure 8.7. Single specimen carbon isotope values. Raw  $\delta^{13}\text{C}$  values, symbol size denotes size fraction, for convenience the data points are offset from one another. Highlighted regions represent the glacial and interglacial Heinrich events (HE14 and HE15) and Termination III.

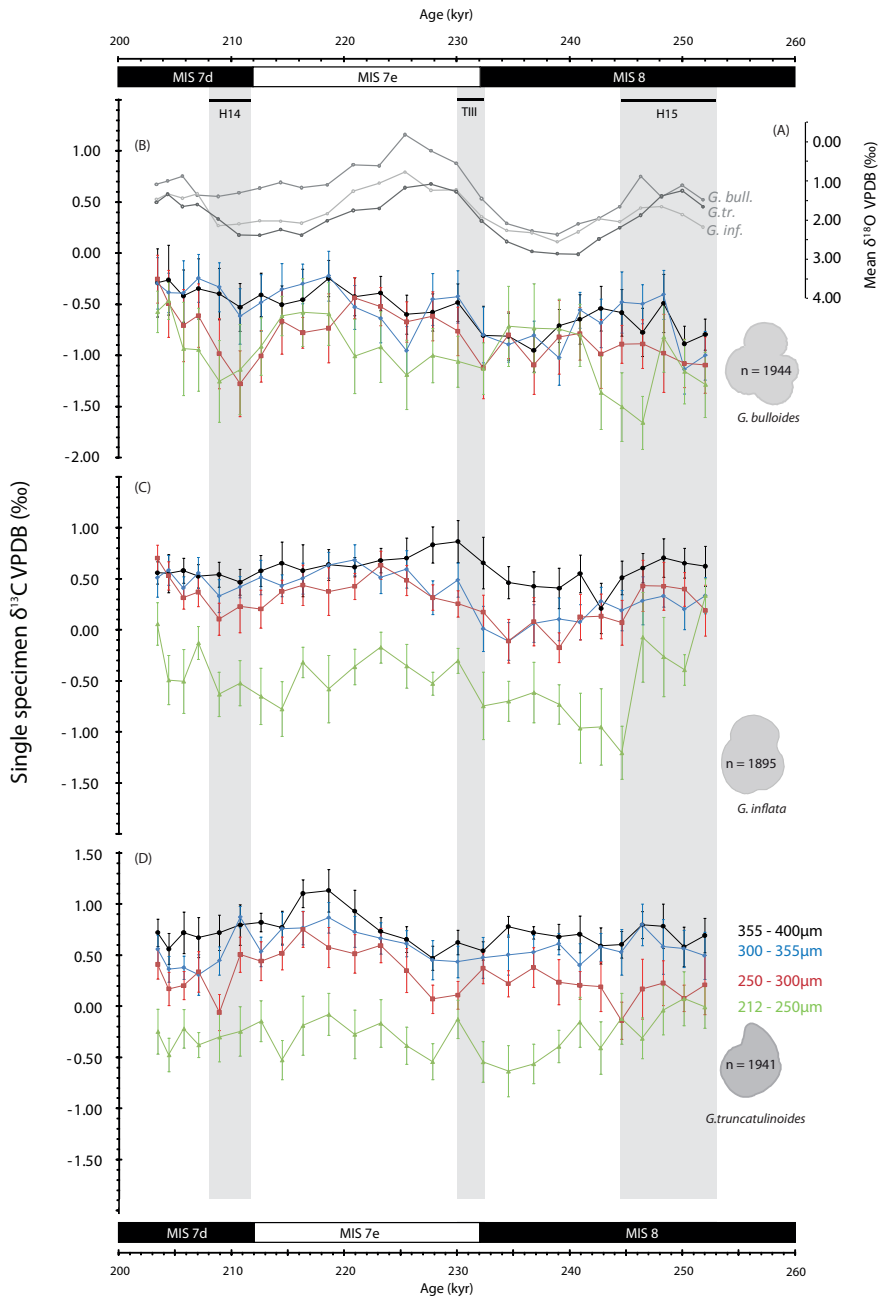


Figure 8.8. Mean carbon isotope values with 95% confidence intervals. (a) For comparative purposes the mean  $\delta^{18}\text{O}$  values for *G. bulloides*, *G. inflata* and *G. truncatulinoides*. Mean  $\delta^{13}\text{C}$  values for (b) *G. bulloides*, (c) *G. inflata* and (d) *G. truncatulinoides*, colour denotes size fraction. Highlighted regions represent the glacial and interglacial Heinrich events (HE14 and HE15) and Termination III.

*G. truncatulinoides*. There are only two samples, out of 26, where the smallest size fraction of *G. bulloides* appears to deviate from the others, i.e. at 244 and 246 kyr (Figure 8.8). In comparison only the samples at 246 and 252 kyr show similar isotope values between all size fractions, while for the rest 212–250  $\mu\text{m}$  is depleted. Between 225–236 kyr - the transition from MIS8 to MIS7 - the largest specimens of *G. inflata*, analysed here (355–400  $\mu\text{m}$ ), become more enriched in  $^{13}\text{C}$  than the other size fractions. For *G. truncatulinoides* in the intervals 208, 230, 240 and 244–252 kyr, the values for the two size fractions 212–250  $\mu\text{m}$  to 250–300  $\mu\text{m}$  overlap. In contrast at 205, 207, 216, and 218 kyr the usually overlapping 300–355  $\mu\text{m}$  to 355–400  $\mu\text{m}$  size fractions deviate, with the larger size fraction becoming more enriched (Figure 8.8). In contrast with  $\delta^{18}\text{O}$ , the  $\delta^{13}\text{C}$  of the means of the smallest sized specimens have a larger range than that of the largest sized specimens, none of the linear regressions are statistically significant, and likewise show a statistical offset from the  $\delta$ -iso line (Table 8.4, Figure 8.6). However, whilst the mean  $\delta^{13}\text{C}$  of

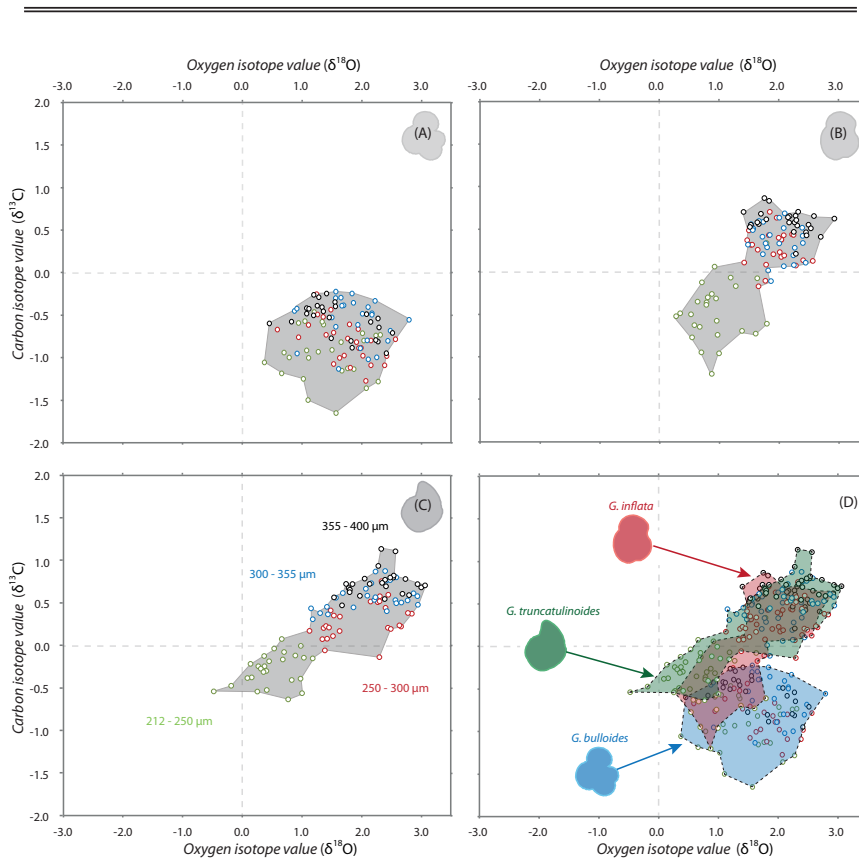


Figure 8.9. Cross-plot of oxygen and carbon values. Cross-plot between mean  $\delta^{18}\text{O}$  and  $\delta^{13}\text{C}$  for all size fractions of (a) *G. bulloides* (b) *G. inflata* (c) *G. truncatulinoides* and (d) all species. For (a–c) symbol colour represents size fraction as per Figure 8.5 and 8.8: 212–250  $\mu\text{m}$  (green), 250–300  $\mu\text{m}$  (red), 300–355  $\mu\text{m}$  (blue) and 355–400  $\mu\text{m}$  (black).

the smallest sized specimens overlap between species, there is a distinct ranking between the largest size fractions with *G. bulloides* having a relatively offset from *G. inflata* and *G. truncatulinoides*.

Statistically, 19 of the *G. bulloides* samples (6 are 90% and 13 are 95% at the confidence level), 24 of the *G. inflata* (3 are 90% and 21 are 95% at the confidence level) and 26 of the *G. truncatulinoides* (26 are 95% at the confidence level) are significant at, and above, the 90% confidence level (Table 8.5). Small (212-250  $\mu\text{m}$ ) specimens of surface dwelling *G. bulloides* and intermediate *G. inflata* have a larger range in mean  $\delta^{13}\text{C}$  than larger specimens (Figure 8.6 and 8.8). Curiously the relationship between size and  $\delta^{13}\text{C}$  is strikingly different from the relationship for  $\delta^{18}\text{O}$ ; the large offset in oxygen between 212-250  $\mu\text{m}$  and 250-300  $\mu\text{m}$  for *G. truncatulinoides* is not visible in the carbon isotope record. The results of the t-test for dependent samples shows that all are statistically significantly different at the 95% confidence level suggesting that the offset between size fractions is not constant (Table 8.5).

### 8.3.4 Covariance

Interdependence between  $\delta^{18}\text{O}$  and  $\delta^{13}\text{C}$  (Table 8.6 and 8.7) is visualised in a cross-plot (Figure 8.9). On average both *G. bulloides* and *G. inflata* show a decreasing correlation coefficient with size between 212 and 355  $\mu\text{m}$ . Both however show a reversal of this trend towards the largest size fraction (355-400  $\mu\text{m}$ ; Table 8.6 and 8.7). The average correlation coefficient shows no variation consistent with changes between the Glacial and Interglacial, although *G. bulloides* shows marginally lower values during HE14, HE15 and TIII, and all species have their lowest correlation coefficient at 250 kyr. *G. bulloides* has considerably more depleted values in  $\delta^{13}\text{C}$  than the other species of planktonic foraminifera whilst smaller specimens of *G. inflata* overlap the area covered by all sizes of *G. bulloides*. Peculiarly, small sized specimens of *G. truncatulinoides* have on occasion more depleted values of  $\delta^{18}\text{O}$  than the other species, for a similar size.

## 8.4 Discussion

### 8.4.1 Size-isotope relationship

In this paper we applied multiple individual specimen analysis (ISA) to the problem of the size-isotope relationship to more than one sample to assess: whether (1) there is a significant correlation between size and stable isotopes, and if so, (2) whether the relationship remains constant through time over a large climatic perturbation, i.e. Glacial Termination-III. Previous studies testing the relationship between shell size and the isotopic signal have shown systematic differences between both oxygen and carbon isotopes [Berger *et al.*, 1978; Billups and Spero, 1995; Kroon and Darling, 1995] (Figure 8.10). This represents a logical partitioning between the isotopes of the two elements carbon and oxygen: Carbon isotopes predominately represent biotic processes such as productivity as a function of metabolic rates and nutrient concentrations, as



R & A

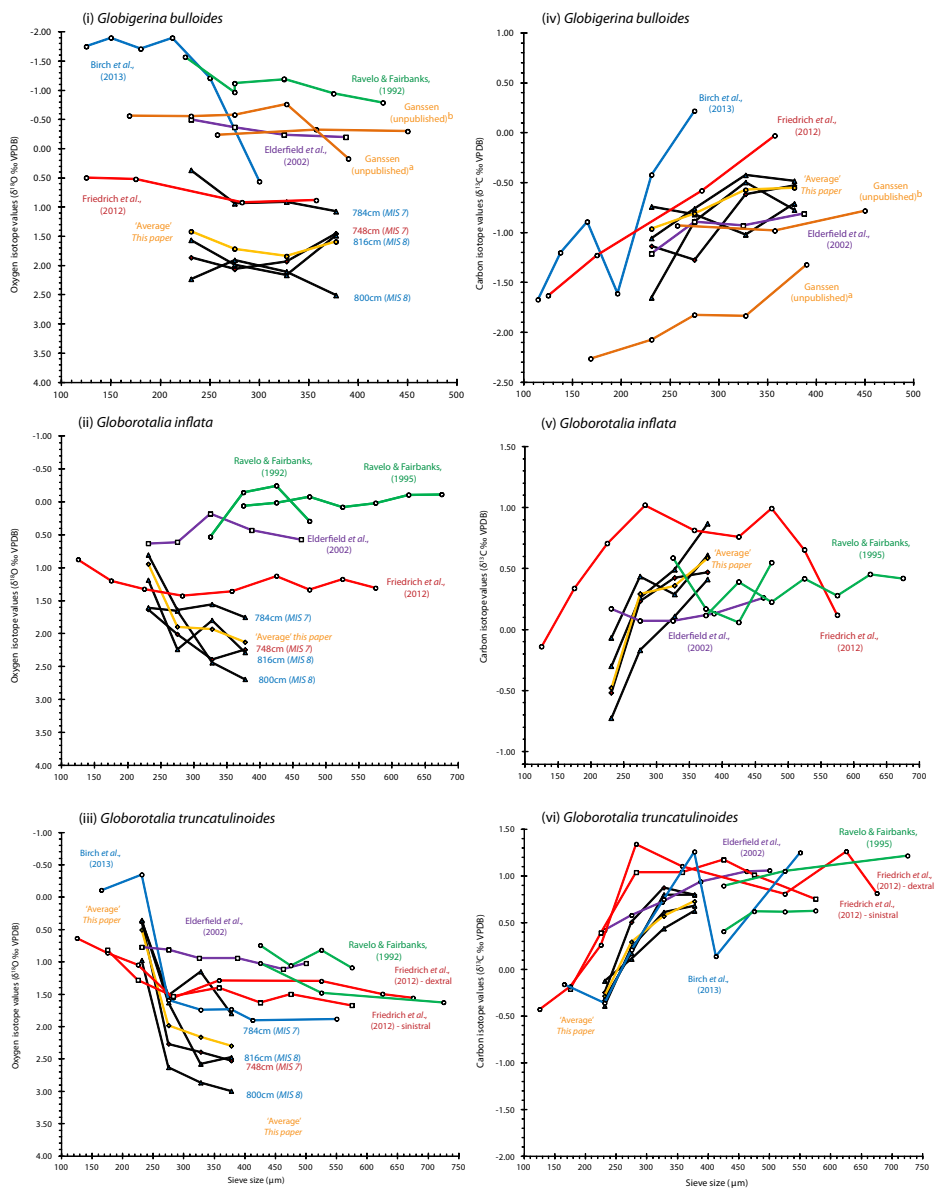


Figure 8.10. Previous size-isotope relationship. Previously published size isotope trends (i-iii)  $\delta^{18}\text{O}$  and (iv-vi)  $\delta^{13}\text{C}$  compared with four samples that represent, based upon the ratio between *Neogloboquadrina pachyderma* and *N. incompta* [Chapter 6] cold and warm periods of MIS 8 and MIS 7. Additionally an average size-isotope was constructed for comparison. Unpublished work of Ganssen is from Indian Ocean core samples.

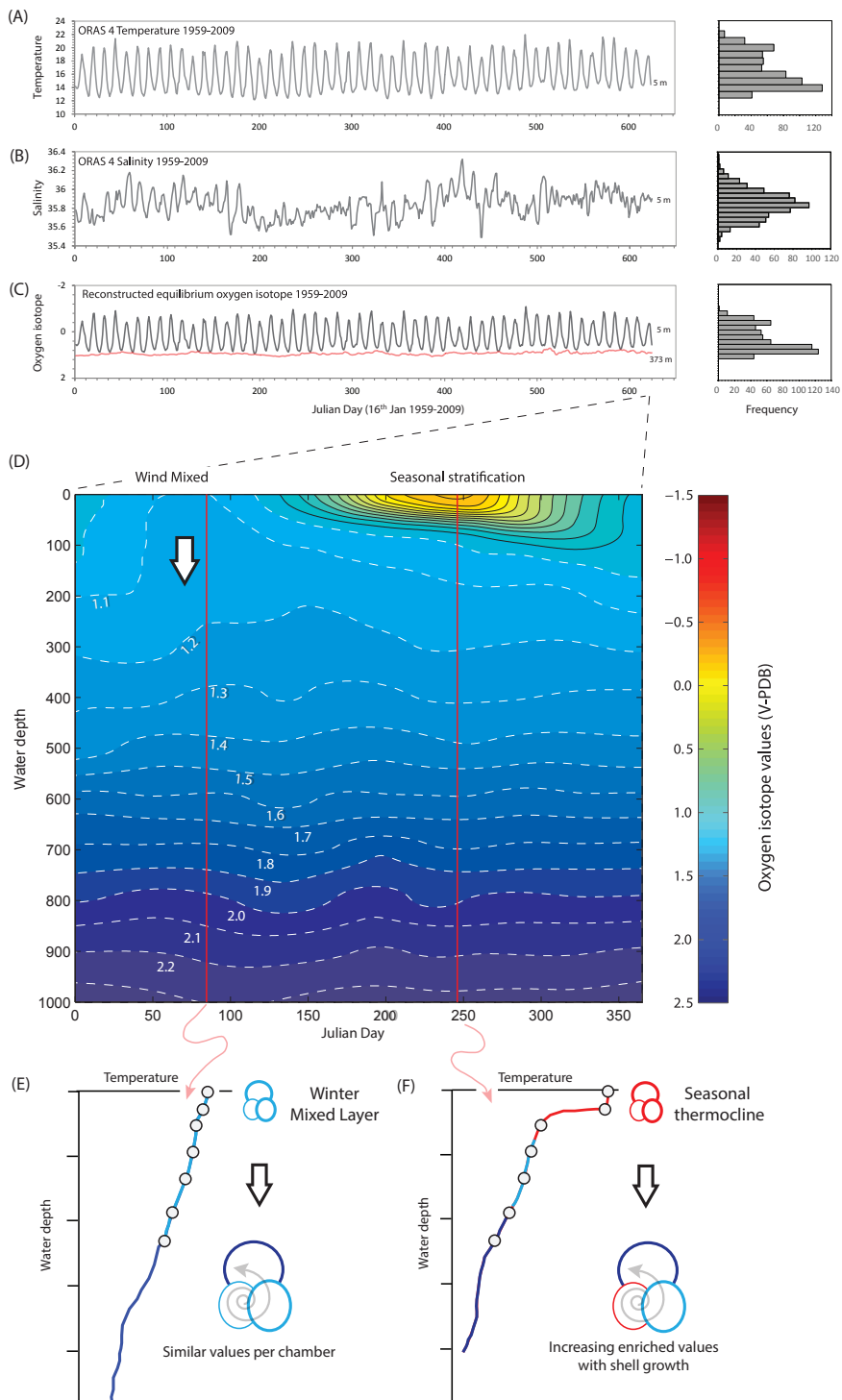
well as being influenced by the photo-auto/heterotrophic symbionts that some species of foraminifera host. They can also represent the abiotic *i.e.* ventilation of oceanic water masses. Oxygen isotope values are primarily influenced by abiotic factors such as glacioeustatic/ice volume, local hydrographic evaporation/precipitation, and temperature. At a cursory glance our results show that larger specimens of both *G. inflata* and *G. truncatulinoides* are enriched in both  $^{18}\text{O}$  and  $^{13}\text{C}$  compared to smaller specimens, although this relationship is only constant for *G. truncatulinoides*. Whilst specimens of *G. bulloides* show no significant variation with size for  $^{18}\text{O}$ , with small and large specimens showing a near identical isotope trend across Termination III, there is a progressive enrichment in  $^{13}\text{C}$  for increasing size. *Berger et al.* [1978] considered that the size-isotope relationship can be broadly grouped into three categories: 1) “normal” in which progressively larger sizes are more enriched, 2) “reversed” in which larger sizes are more depleted and 3) “mixed” in which no clear trend can be deduced, for both  $\delta^{18}\text{O}$  and  $\delta^{13}\text{C}$ . The results presented here show that *G. bulloides* and *G. inflata* vary between “normal” and “mixed”, whilst only *G. truncatulinoides* shows a consistent “normal” trend (see Supplementary figures 1-6).

With respect to the “normal” trend *Berger* [1979] considered four possible explanations for an enrichment in oxygen isotope composition with increasing size: (i) size is related to physical parameters, *i.e.* temperature [*Schmidt et al.*, 2006] and thus larger specimens relate to optimum conditions [*Bé and Lott*, 1964; *Bé et al.*, 1966; *Berger*, 1971]; (ii) the degree of disequilibrium in calcification changes with growth [*Vergnaud-Grazzini*, 1976] and/or physical parameters (*i.e.* temperature); (iii) growth related depth change - with smaller individuals being found in greater concentrations closer to the surface - the implication being that small shells are prematurely (*i.e.* pre-reproduction) terminated individuals [*Emiliani*, 1954a; 1971]; (iv) adults that sink but do not reproduce continue to calcify giving a more enriched signal (Figure 8.11). “Mixed” trends however pose a problem in explaining oxygen isotopes solely related to growth related depth change. Consider that the transition from juvenile-neanic to adult stages occurs between 100 and 200  $\mu\text{m}$  [*Brummer et al.*, 1987], then all specimens above 200  $\mu\text{m}$  are adult. The shape of the size frequency distribution of the pre-adult population is exponential whereas in comparison the adult population has a distinct Gaussian shape [*Brummer et al.* 1986, 1987; *Peeters et al.*, 1999], which suggests that adult specimens that are larger than the mean should be considered giants and on the contrary smaller specimens as dwarfs [*Berger*, 1971]. It has been shown that tropical species increase in size with warmer waters, whereas polar species are larger in colder waters [*Stone*, 1956; *Kennett*, 1968; *Bé et al.*, 1973; *Hecht*, 1974; *Hecht et al.*, 1976; *Schmidt et al.*, 2006], favourable conditions between seasons may explain a “mixed” signal. The oxygen isotope data presented in this paper will be discussed with respect to these possibilities in the following sections.



R &amp; A





### 8.4.2 Size of planktonic foraminifera

Whilst the faunal transition from the glacial MIS8 to interglacial MIS7 shows the characteristic pattern associated with a warming climate and despite a moderate increase in size occurring during the glacial period (234 – 252 kyr; Figure 8.3) the changes in abundance are not concurrent in size or magnitude, with any variation in the isotopic composition in *G. bulloides* between size fractions. Likewise no pattern can be discerned in either *G. inflata* or *G. truncatulinoides* which whilst displaying a (predominately) statistically significant isotopic offset between the difference size fractions and/or change in average size through time are not correlatable. If one considers that the modern size of foraminifera is related to a number of factors, including: temperature and productivity, then the modern size of foraminifera is related to the modern oceanographic regime. At present this regime is composed of a cyclonic and anti-cyclonic gyre system, controlling and maintaining the continued existence of the associated water masses. During glacials the North Atlantic is surrounded by continental ice sheets which are inferred to occur down to the 40°N in the west and 50°N to the east [McIntyre *et al.*, 1976] as such no analogue to the mixing of water masses synonymous with the modern Gulf Stream-North Atlantic Drift water via cyclonic and anticyclonic eddies [McIntyre *et al.*, 1976] occurs, as polar water masses extended as far south as 45°N. In the modern ocean *G. bulloides* has its largest size occurring at 50°N, if one is to consider that a compression or elimination of certain transitional water masses occurs during glacial periods then this maximum size should be centered at or to the south of the location of the studied core, *i.e.* a size decrease should be observable at our core location. However, the control on size is not as clearly known for non-symbiotic species as it is for symbiont bearing species, whilst temperature may play an important role the dynamics of the upper water column such as the strength of winter mixing or the Spring transition from a well-mixed to stratified water column has been linked to certain seasonal successions

Figure 8.11. (opposite page) Schematic diagram of the key hydrological parameters at the core site and the insolation pattern for the studied interval. Ocean reanalysis dataset of (a) Monthly temperatures and (b) Monthly salinity at 5 m water depth for the years 1959-2009, excluding the warming since 2009 [Balmaseda *et al.*, 2013]. Using (a) and (b) the (c) oxygen isotope equilibrium was calculated for 5 m (black line), for reference (red line). (d) Oxygen isotope equilibrium ( $\delta^{18}\text{O}_{\text{eq}}$ ) representing the water structure plotted against time based upon ‘an average year’ using values of World Ocean Atlas (WOA09) extracted from Ocean Data View (ODV). The main foraminiferal flux, as determined by the North Atlantic Bloom Experiment (NABE) the initial pilot study of the Joint Global Ocean Flux Study (JGOFS), lies between March and July. Maximum insolation occurs in June however the warmest month is later in September/October. Estimated depth habitat of *G. bulloides*, *G. inflata* and *G. truncatulinoides* is 100 m, 400 m and 800 m respectively. Schematically, foraminifera that calcify in (e) the Winter mixed layer are likely to record similar values for each successive chamber in comparison with those foraminifera that calcify in the (f) seasonal thermocline.



R & A

between species [Wolffreich, 1994; Ganssen and Kroon, 2000; Salmon *et al.*, 2014]. In the modern North Atlantic, late Winter deep mixing supplies the surface layer with on average approximately 8  $\mu\text{mol/l}$  of nitrate and 6  $\mu\text{mol/l}$  of silicate, the rise in insolation triggers the develop of the thermocline that in combination with rapidly shoaling nutricline into the euphotic zone generates the spring bloom of phytoplankton [Broerse *et al.*, 2000]. For the modern ocean a proxy for stratification, introduced by Lototskaya and Ganssen [1998], was deduced for a north-south transect of box-core tops in the North Atlantic [Ganssen and Kroon, 2000]. Based upon the investigation of the modern latitudinal variability in planktonic foraminiferal stable isotopes they observed that *G. bulloides* dwells at a shallower depth than *G. inflata*. Hence, the difference ( $\Delta\delta^{18}\text{O}$ ) between these surface and subsurface dwellers can be converted into an approximate temperature difference by taking into account that a change of approximately -0.22‰ occurs per °C increase. When this difference equals (or approaches) zero, such as for example occurring in the modern ocean at approximately 58°N, the water column was mixed down to the permanent thermocline, while higher values indicate a stratified water column [Ganssen and Kroon, 2000]. Through the estimation of the strength of stratification, the intensity of the spring bloom can be deduced. Feldmeijer *et al.* [Chapter 6] estimate that during the glacial the ocean is well mixed, becoming stratified at the termination, before transitioning toward a well-mixed water column during the climate minima of MIS7d. Faunal and geochemical data between MIS9 and MIS7 suggests that a sharp temperature gradient existed between the North Atlantic ocean (55°N) and the Nordic Seas (68°-76°N) [Ruddiman and McIntyre, 1976; Ruddiman *et al.*, 1986; Bauch, 1997], as a result of a relatively minor ingress of warm Atlantic surface water into the Nordic Sea. The deviation from an expected size decrease for both *G. bulloides* and *G. inflata*, due to a reduction in temperature at the glacial, may have been counter balanced by a more productive water column.

### 8.4.3 Depth habitat

Planktonic foraminifera, as pelagic organisms, can be considered to have optimal conditions that are both geographic and vertical. The fact that the expected size decrease in relation to the geographic movement of the oceanic fronts appears to not occur could also have some relation to changes in depth habitat. The depth habitat of planktonic foraminifera has long been considered to relate to temperature [Emiliani, 1954a], although later related to the specific thermal structure *i.e.* stratification of the water column [McKenna and Prell, 2004], development of the thermocline, the depth and development of the chlorophyll maximum zone, food availability, *i.e.* phytoplankton and the depth of light penetration [Caron *et al.*, 1981; Hemleben *et al.*, 1989]. Different ecological niches are associated with differences in the depth habitat. Spinose species for example are commonly associated with both a shallower depth habitat and symbionts that act as important food source in oligotrophic conditions. Depth habitat reconstructions, calculated via abundance counts of plankton tows and/or the isotopic composition of sedimentary material, have placed the species

analysed as distinct ecological niches associated with ‘shallow’, ‘intermediate’ and ‘deep’ depths, for *G. bulloides*, *G. inflata* and *G. truncatulinoides* respectively.

*Hemleben and Spindler* [1983] reported that the preferred depth habitat of *G. bulloides* is between the surface mixed layer and 200 m. Both *Bé* [1977] and *Deuser and Ross* [1989], however, suggested a shallower depth habitat of 50-100 m and 25-50 m, respectively. The species depth habitat appears strongly controlled by the distribution of particulate food. The Deep Chlorophyll Maximum (DCM) is often associated with high(er) abundance of this species and since the DCM may be found at different depths, although predominately at the base of the surface mixed layer, one can expect this species to follow the food rich levels in the water column. Seasonal variability in the depth habitat may account for this discrepancy between authors. Based upon plankton tow sampling *Ottens* [1992b] ascribed a greater depth (0-100 m) in April than in August (0-50 m). Whereas, the non-spinose *G. inflata* is considered to be an intermediate to deeper dwelling species, typically associated with the base of the seasonal thermocline [*Cléroux et al.*, 2008; *Cléroux et al.*, 2007; *Ganssen and Kroon*, 2000; *Groeneveld and Chiessi*, 2011; *Lončarić et al.*, 2006] associated with subpolar to subtropical water masses [*Bé*, 1969; *Farmer et al.*, 2011; *Ganssen and Sarnthein*, 1983; *Thiede*, 1971, 1975]. In the South Atlantic, for instance, *G. inflata* reaches its highest relative abundance in the transitional waters of the subtropical and sub-Antarctic regions at water temperatures between 13-19°C. However, it has been shown to dominate the lower temperature (2-6°C) sub-Antarctic region in South Pacific [*Bé*, 1969]. Calcification, however, occurs from the mixed layer down to water depths of 500-800 m [*Hemleben and Spindler*, 1983; *Wilke et al.*, 2006]. Narrower depth intervals have been proposed for both the North Atlantic, at 0-150 m [*Ottens*, 1992b] and 300-400 m [*Elderfield and Ganssen*, 2000], and the South Atlantic at 50-300 m [*Mortyn and Charles*, 2003]. The non-spinose species *G. truncatulinoides* has a dimorphic coiling provincialism (dextral and sinistral) although it is considered to inhabit a deep depth, approximately down to ~800 m or even deeper [*Hemleben et al.*, 1985; *Lohmann*, 1992; *Lohmann and Schweitzer*, 1990] where they are considered to secrete a secondary ‘gametogenetic’ crust [*Bé and Ericson*, 1963; *Hemleben et al.*, 1985]. Given the considerable depths it inhabits it likely feeds on detritus settling from the photic zone. Its morphology, more explicitly the height of the conical shell, has changed temporally and spatially [*Lohmann*, 1992 and references therein] with different populations having different isotopic compositions [*Williams et al.*, 1988]. *Fairbanks et al.* [1980] found, using plankton tows, that this species is enriched isotopically, compared to equilibrium values, when found above the thermocline, in equilibrium on the thermocline and depleted below it. This deviation is likely caused by offsets between primary and secondary crusts [*McKenna and Prell*, 2004; *Mulitza et al.*, 1997; *Vergnaud Grazzini*, 1976], although this may be a seasonal-encrusting artefact [*Spear et al.*, 2011]. Our results show that species with a larger modern depth habitat, such as globorotalids, have for the most part a statistically significant offset between smaller sized and larger sized specimens in the sedimentary record. With increasing water depth, oxygen isotope equilibrium

1

2

3

4

5

6

7

8

9

R &amp; A

values become successively more enriched (Figure 8.11), considering that size and depth are linked then our results parallel the work of *Williams et al.* [1981] and the later work of *Lončarić et al.* [2006] in suggesting that the  $\delta^{18}\text{O}$  of smaller sized (predominately globorotalid) foraminifera record upper ocean/surface conditions. During the descent through the water column foraminifera add new calcite, their shell's geochemical composition is therefore an integrated history of the hydrology at different water depths [*Hemleben and Bijma*, 1994; *Wilke et al.*, 2006] (Figure 8.11).

#### 8.4.4 Seasonality

The isotopic composition of larger specimens represents continuous calcification through the water column to deeper waters with lower temperatures, thus giving isotopically enriched values. Given the overlap of the larger than  $>250\ \mu\text{m}$  in all species it is possible that no size-depth stratification occurs after a given growth stage. Although given that the seasonal temperature variation with depth is small ( $<1^\circ\text{C}$  for 200 m,  $<0.6^\circ\text{C}$  for 500 m) different sizes may represent growth in different seasons with varying ecological constraints. However, the “mixed” signal, for instance at 214.5 kyr for *G. bulloides* where both small and large specimens have the same  $\delta^{18}\text{O}$  would suggest a seasonal effect. The modern seasonal temperature range at the core site is  $10\text{--}12^\circ\text{C}$ , assuming that a change of 1‰ corresponds to a  $4^\circ\text{C}$  then the amplitude of the seasonal temperature signal alone is approximately 2.5–3.0‰. This is further complicated by potential changes attributable to evaporation and precipitation and the occasional-intermittent presence of freshwater pulses, as the core site is situated within the ice rafted debris belt [*Hodell and Curtis*, 2008]. If we consider that the isotope values of 250–355  $\mu\text{m}$  occurs during favourable conditions, the two end members (212–250 and 355–400  $\mu\text{m}$ ) could occur during unfavourable conditions during the height of summer when the water column is strongly stratified. Curiously, the average correlation coefficient between  $\delta^{18}\text{O}$  and  $\delta^{13}\text{C}$  shows a reversal in its decrease with size trend in this larger size fraction (355–400  $\mu\text{m}$ ) which may support this seasonal explanation, although it may also be a change in vital effect or metabolic dominance of the isotopic signal.

Intriguingly there are a number of instances where the smallest specimens of *G. inflata* have similar values as larger specimens ( $>250\ \mu\text{m}$ ) these events occurring halfway between insolation minima and maxima, apart from at 234–239 kyr during the onset of the termination. Were it to be a shoaling of the depth habitat then larger specimens would be expected to show similar values to smaller specimens and not the other way around. The fact that these values show a relationship with  $\delta^{18}\text{O}_{355-400\mu\text{m}}$  *G. bulloides* ( $r = 0.7025$ ;  $n = 8$ ) suggests a modification of the structure of the upper ocean. The biological vertical structure of the water column is dependent upon the amount of incidental light, notwithstanding surface ocean processes such as surface layer mixing (Figure 8.11d–f). In the modern ocean the average wind velocity increases between November and February which mixes the ocean down to depths of 150–300 m

[Broerse *et al.*, 2000]. The penetrative depth of sunlight, and thus the surface available to direct heating, is greater in the ocean (~100m) than on land (~1-2 m) accordingly temperature change in the ocean is distributed over a larger area than on land which has a lower capacity to either conduct or store heat. Variation in the ocean-land heat contrast directly affects the influence of wind strength in the region and thus the strength of wind driven turbulence that mixes the upper ocean. The fact that these events occur halfway between a minima and maxima in insolation may suggest that the wind regime over this region of the North Atlantic is particularly sensitive to the reduction in extremes. Likewise, the shift in both the relative abundance (Figure 8.3) and the oxygen isotopic standard deviation (Supplementary Figure 8.7) of *G. bulloides* corresponds to a change in the insolation difference between the vernal Equinox and the summer Solstice (e.g. between March and June) ( $r = 0.5748$ ;  $n = 26$ ). This means that, when the difference between the two seasons is greatest the growing season is reduced, thus the surface species has a 'reduced' range of values. It is postulated that during periods of reduced seasonality the stratification that exists in the summer months was not as strong as it is today.

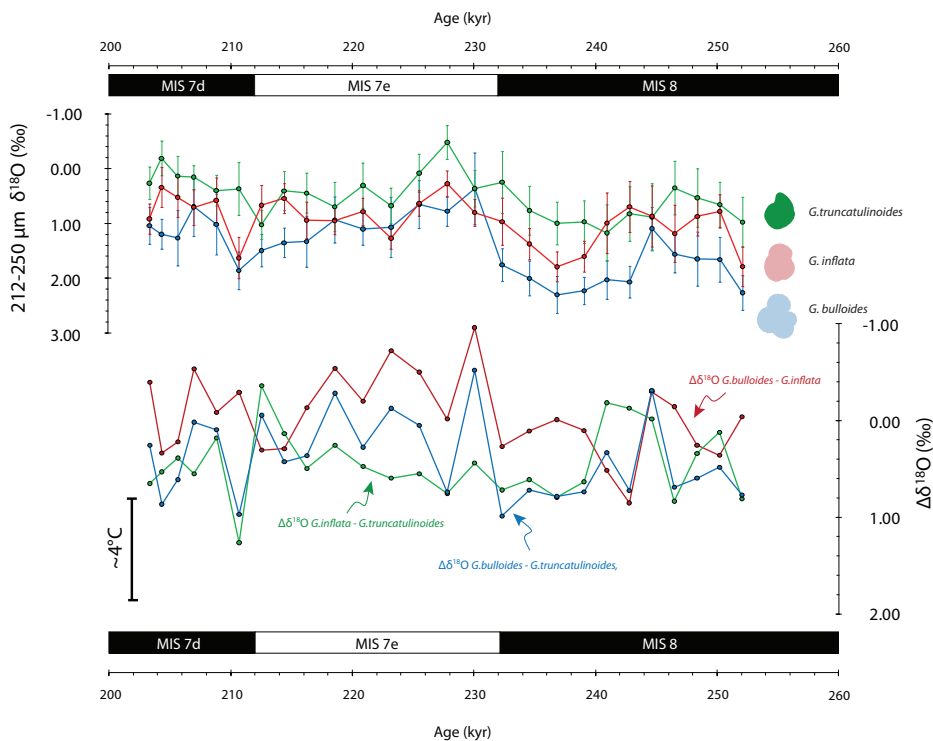


Figure 8.12. Oxygen isotope of smallest size fraction and differences. (a) The oxygen isotopes between small sized specimens of *G. bulloides*, *G. inflata* and *G. truncatulinoides* and (b) the calculated difference between species ( $\Delta\delta^{18}O$ ).





### 8.4.5 $\Delta\delta^{18}\text{O}$ between species

Oxygen isotopes between similar sizes of different species show differences between small specimens (212–250  $\mu\text{m}$ ) of the deep-dwelling *G. truncatulinoides*, and the surface dwelling *G. bulloides*, of up to 1.3 ‰  $\Delta\delta^{18}\text{O}$  (corresponding to  $\sim 5^\circ\text{C}$ ) during some periods, although on average this offset is smaller at  $\sim 0.5$  ‰ or  $2^\circ\text{C}$  (Figure 8.12). This pattern can be accomplished by: (1) differences in  $\delta^{18}\text{O}$  fractionation factors between species confirmed by numerous authors [Curry and Matthews 1981; Duplessy *et al.*, 1981; Fairbanks *et al.*, 1980; Shackleton, 1974; Shackleton *et al.*, 1973; Vergnaud-Grazzini, 1976; Williams *et al.*, 1979]; (2) calcification in a water mass with a different ambient  $\delta^{18}\text{O}_{\text{eq}}$ , *i.e.* convection and sinking of isotopically depleted water [Macdonald *et al.*, 1995] during sea ice formation [Rohling and Bigg, 1998; Strain and Tan, 1993]; (3) expatriation of more southerly grown specimens via a proto-gulf stream deflected by a southerly Polar Front [Cifelli and Smith, 1970; Lototskaya and Ganssen, 1999; Phleger *et al.*, 1953; Weyl, 1978]; or (4) calcification in distinct seasons. Explanation (ii) that calcification occurs in a water mass with a different  $\delta^{18}\text{O}_{\text{sw}}$  is plausible. For instance during sea ice formation surrounding water masses become isotopically depleted as the  $\delta^{18}\text{O}$  of sea ice is  $2.57 \pm 0.10$  ‰ enriched relative to the isotopic composition of sea water [Macdonald *et al.*, 1995]. The formation of which increases surface ocean salinity enough to lead to convection and sinking of this depleted water mass [Rohling and Bigg, 1998; Strain and Tan, 1993]. This depleted water mass is replaced by surface waters (to some degree) unaffected by the freezing process [Rohling and Bigg, 1998] meaning that species that calcify during sea ice formation will have a more depleted signal. Similarly the core site is situated within the ice rafted debris belt [Hodell and Curtis, 2008; Park, 1998] indicating that this area would have been affected by meltwater during certain periods of the year. However, both of these hypotheses cannot satisfactorily explain the continuation of this phenomena in shallower ‘interglacial’ depths of the core.

Explanation (3) finds support from observations of Phleger *et al.* [1953] that low latitude faunas are circulated northwards in the western portion of the Atlantic basin, whereas high latitudes faunas are displaced southwards in the eastern basin, as dictated by the clockwise direction of the currents within the North Atlantic gyre (Figure 8.1). The large difference between the fine fractions of *G. bulloides* and *G. truncatulinoides* (up to 1.3‰) cannot account for differences in calcification depth alone as it would indicate a deeper calcification for *G. bulloides*. Instead calcification at a more southerly and warmer location is plausible. During glacial conditions the biogeographic distribution of this species contracts to lower latitudes as the boundary of the Polar Front moves southwards down to the latitude of the Iberian margin. Expatriates carried by the proto-Gulfstream would have been deflected along the polar front [Lototskaya and Ganssen, 1999; Weyl, 1978] into this core-location as deduced by the IRD belt [Berger and Jansen, 1995; Ruddiman and McIntyre, 1981]. Cifelli and Smith [1970] through releasing drift bodies from eastern North America indicated that surface currents could



redistribute organisms when they collected these same drift bodies in the Azores. It is possible that the more depleted in  $\delta^{18}\text{O}$  specimens represent the endemic population, and the more enriched specimens are expatriates [Lototskaya and Ganssen, 1998]. Were these expatriates to emigrate into unfavourable conditions they may not have grown additional chambers in equilibrium with the ambient conditions and thus an observable offset would occur.

Both (2) and (3) can be discounted given that the phenomenon occurs irrespective of oceanic mode (i.e. glacial-interglacial). Given the seasonal flux [Tolderlund and Bé, 1971] this isotopic difference could relate to deep-sea sediments being composed of specimens from species that potentially calcify during different seasons [Williams *et al.*, 1979], therefore requiring no problematic large scale transport. Tolderlund and Bé [1971] based upon four years of seasonally collected plankton tows at weather station Delta (44°00'N, 41°00'W) considered that *G. bulloides* had a continuous flux throughout the period of November to August, while both *G. inflata* and *G. truncatulinoides* show two flux maxima, one between December and March and between December and January respectively. This relates to temperatures during this time window of between 10-23°C for *G. bulloides*, 10-23°C for *G. inflata* and 8-22°C *G. truncatulinoides*. Whilst these temperature distributions suggest that *G. truncatulinoides* occurs in colder waters the optimum temperatures of these species are 10-12°C, 10-17°C and 15-18°C, respectively, consistent with the idea of calcification in warmer temperatures [Tolderlund and Bé, 1971]. *Globigerina bulloides* has highest fluxes during the spring bloom prior to stratification of the water column were *G. truncatulinoides* to calcify later in the year, at the base of the thermocline, then it would explain the deviation in isotopic composition between the two species.

#### 8.4.6 Carbon isotopes

In comparison with oxygen isotopes there is generally an enrichment in  $^{13}\text{C}$  with size, synonymous with previous studies [Franco-Fraguas *et al.*, 2011], as per the “normal” trend [Berger *et al.*, 1978]. Changes in the  $\delta^{13}\text{C}$  values of planktonic foraminifera have invoked photosymbiosis [Spero and DeNiro, 1987], metabolic fractionation i.e. respiration [Berger *et al.*, 1978], diet [DeNiro and Epstein, 1978] and metabolic and/or symbiotic influences on the ambient and internal carbon pool (i.e. carbonate ion concentration). It is self-evident that the same depth related size- $\delta^{18}\text{O}$  trends are not applicable to carbon isotopes, given the vertical structure of  $\delta^{13}\text{C}$  DIC which as a consequence of the surface photosynthesis and the oxidation of organic matter at depth the isotopic composition of dissolved inorganic carbon ( $\text{DIC} \equiv \Sigma\text{CO}_2$ ) varies vertically resulting in depleted isotopic values at depth as opposed to an enrichment. As photosynthesis preferentially favours uptake of  $^{12}\text{C}$  organic matter produced through this pathway has typical  $\delta^{13}\text{C}$  values of between -20 to -25 ‰, as a result the DIC at the surface, in the photic zone, is enriched in  $\delta^{13}\text{C}$  by approximately ~2 ‰. As the isotopically depleted organic matter sinks it is oxidised lowering the ambient  $\delta^{13}\text{C}$  value to approximately ~0 ‰. The calcification depth surmised from using  $\delta^{13}\text{C}$ , when



R & A

compared with the modern  $\delta^{13}\text{C}_{\text{DIC}}$  vertical profile [Chapter 6], would indicate a shallower depth habitat. Our results however show that the relative enrichment between species is consistent with the depth habitat per se, *i.e.* deeper dwellers have a larger enrichment than shallower dwellers (Figure 8.9d). This discrepancy could relate to either a (i) temperature related fractionation, (ii) diet and/or (iii) the addition of a secondary crust. Species specific temperature dependent fractionation is likely caused by the influence of temperature on the physiological rates of the organism, for instance a number of authors have demonstrated that over small temperature ranges the metabolic rate increased exponentially [Bijma *et al.*, 1990; Ortiz *et al.*, 1996]. The change in  $\delta^{13}\text{C}$  per degree Celsius for *G. bulloides* has been estimated experimentally as  $-0.11\text{‰ }^{\circ}\text{C}^{-1}$ , whereas for the symbiotic species *Orbulina universa* it is 2-3 times less in the opposite direction 0 to  $+0.05\text{‰ }^{\circ}\text{C}^{-1}$  [Bemis *et al.*, 2000]. It is noteworthy to point out that for the non-symbiotic species *G. bulloides* this temperature effect will diminish the effect of higher glacial  $[\text{CO}_3^{2-}]$  [Bemis *et al.*, 2000]. Spero *et al.* [1997] through culturing experiments in which *G. bulloides* was grown at constant DIC showed that there is a strong dependence,  $-0.012\text{‰}/(\mu\text{mol kg}^{-1})$  on  $\delta^{13}\text{C}$ , with  $[\text{CO}_3^{2-}]$ . This strong dependence, a consequence of both kinetic and metabolic fractionation factors [Bijma *et al.*, 1999], is species specific [Peeters *et al.*, 2002; Wilke *et al.*, 2006]. In the natural environment the  $[\text{CO}_3^{2-}]$  varies regionally as the solubility of  $\text{CO}_2$  is temperature dependent and vertically as organic matter is remineralised and the subsequent  $\text{CO}_2$  is released and hydrolysed. A 0.5 pH decrease at the shallow oxygen minimum zone for instance would account for a 1 ‰ enrichment in  $\delta^{13}\text{C}$  for those species that inhabit it [Birch *et al.*, 2013]. This sinking organic matter may also contribute to changes in the  $\delta^{13}\text{C}$  of test calcite through changes in food source, feeding efficiency and diet. DeNiro and Epstein [1978] highlighted the fact that consumers are slightly enriched in  $\delta^{13}\text{C}$  from the composition of their food with each trophic level raising the  $\delta^{13}\text{C}$  a process termed cumulative fractionation by McConnaughey and McRoy [1979a; 1979b]. Carnivorous foraminifera are likely to have more enriched values than herbivorous foraminifera. Likewise Hemleben and Bijma [1994] suggested that dietary change between juveniles grazing on phytoplankton or feeding on detritus and the carnivorous diet of later neanic and/or adult stages should coincide with an increase in  $\delta^{13}\text{C}$ . Growth rate, final size,  $\delta^{13}\text{C}$  and rate of chamber addition have all been shown to correlate positively with increased feeding rate [Bé *et al.*, 1981; Bijma *et al.*, 1992; Hemleben *et al.*, 1987; Ortiz *et al.*, 1996], *i.e.* a doubling in feeding rate resulted in a decrease in  $\delta^{13}\text{C}$  by 1 ‰ for specimens of the symbiont bearing *Globigerinella siphonifera* [Hemleben and Bijma, 1994]. As metabolic rates slow down during ontogeny the test becomes more isotopically enriched as the incorporation of light carbon decreases [Bemis *et al.*, 2000; Berger *et al.*, 1978; Birch *et al.*, 2013; Fairbanks *et al.*, 1982; Oppo and Fairbanks., 1989; Spero and Lea, 1996; Vincent and Berger, 1981]. Younger (or smaller) foraminifera are inferred to have higher respiration rates (high metabolic rate thus increased kinetic fractionation) which during calcification leads to a greater amount of metabolic  $\text{CO}_2$  depleted in  $^{13}\text{C}$  incorporated into the test calcite [Bemis *et al.*, 2000; Berger *et al.*, 1978; Ravelo and Fairbanks, 1995]. The addition of a secondary crust, or gametogenetic calcite,

at depth potentially via absorption and remineralisation of earlier chambers and spines during preparations for reproduction may lead to an isotopic offset [Hemleben *et al.*, 1989; Schiebel and Hemleben, 1995]. When restricted to primary calcite Lohmann [1995] discerned there was no size- $\delta^{13}\text{C}$  trend however, as noted by Birch *et al.* [2013] this mechanism would result in depleted values not the enriched values observed.

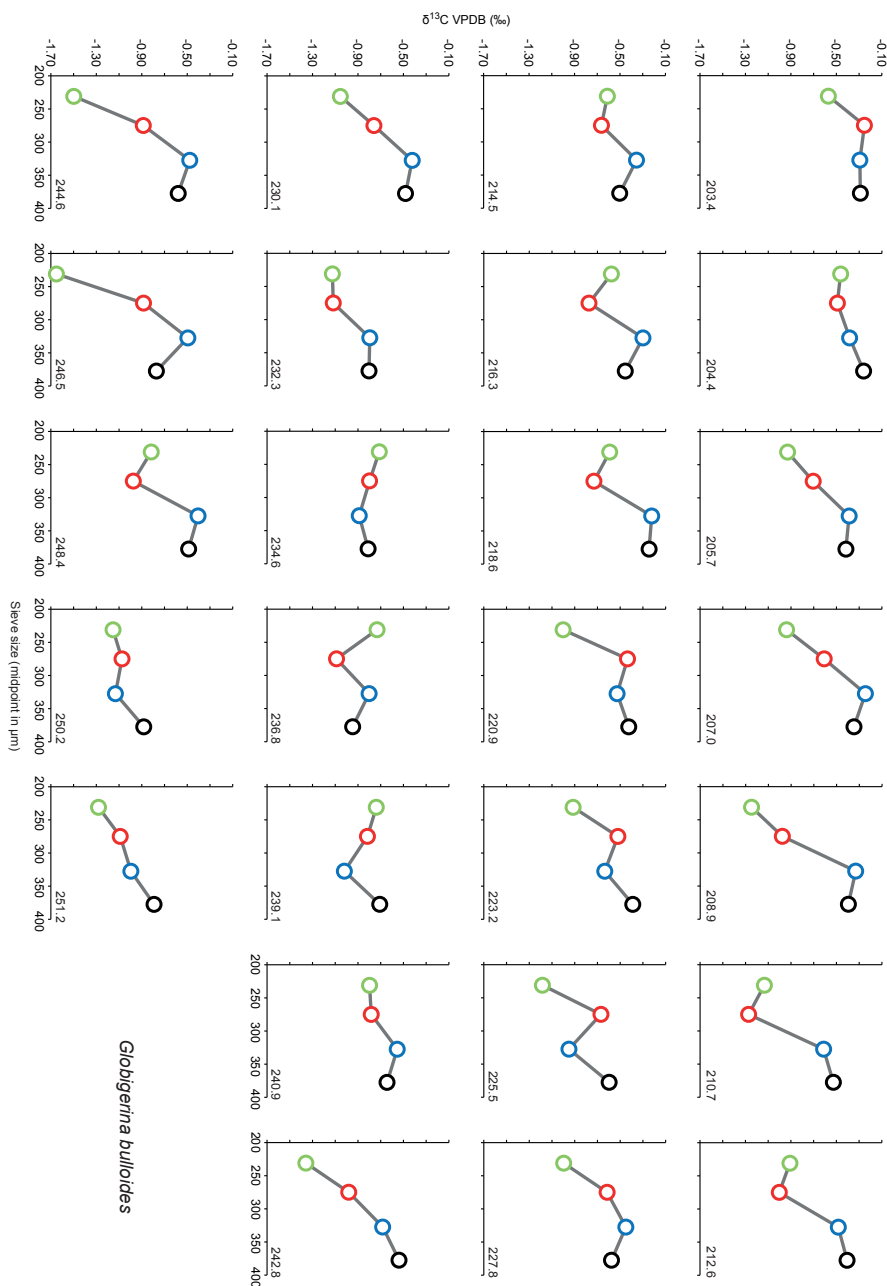
## 8.5 Conclusion

Oxygen isotopic analysis of specimens from different size fractions reveal that for globorotalids smaller shells are isotopically depleted compared to larger shells, whilst we did not find a systematic difference between  $\delta^{18}\text{O}$  of *G. bulloides* in different size fractions. This depletion is inferred to be an effect of different depths inhabited during ontogeny, with smaller specimens calcifying in the warmer shallower surface waters prior to migrating to depth. A large offset between small and larger specimens of *G. truncatulinoides* can be explained by calcification during a warmer season at a shallower water depth. Carbon isotopes show a greater degree of variability, which is inferred to relate to changes in metabolism. Differences between size fractions appear not constant temporally or even spatially as shown by the difference between the data presented here and previously published. This is likely the reason for the lack of a resolution in the literature between studies pertaining to decide on a preferred / recommended size fraction for isotopic analysis. Our results would suggest that 300-355  $\mu\text{m}$  would serve this purpose, however we would caution against using a 'one-size fits all' approach given the seasonal structure of the water column and seasonal succession of species at this core location. Further studies are needed to understand how this size-isotope relationship varies in regions with reduced seasonality, more/less stable and unstable water column dynamics and during transient events, for example associated with sapropel layers.

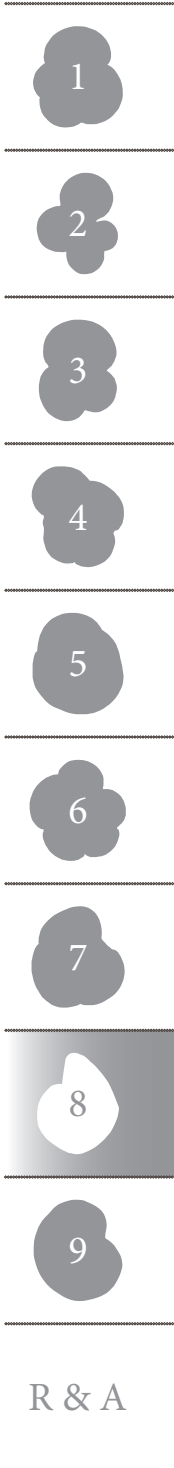
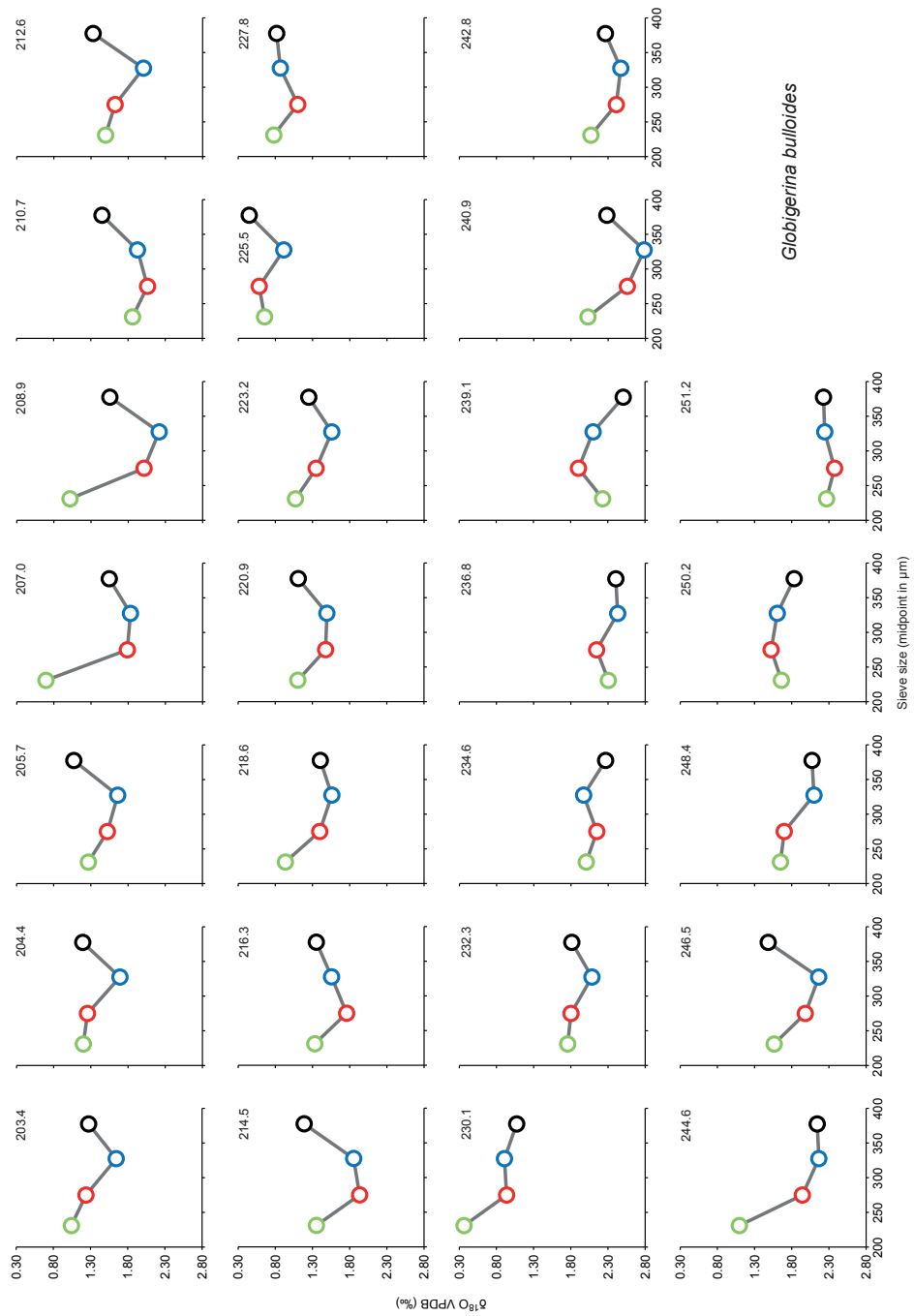
## Acknowledgements

This paper is a contribution to the European 7<sup>th</sup> Framework Project, EPOCA (European Project for Ocean Acidification; FP7/211384), the Darwin Center for Biogeosciences Project 3040 'Sensing Seasonality' and the NWO funded project "Digging for density" (NWO/822.01.0.19). Financial assistance was also provided to the lead author by the VU University Amsterdam. Piston core T90-9p was taken during a joint JGOFS - APNAP expedition aboard the R/V Tyro funded by the Nederlandse Organisatie voor Wetenschappelijk Onderzoek (NWO).

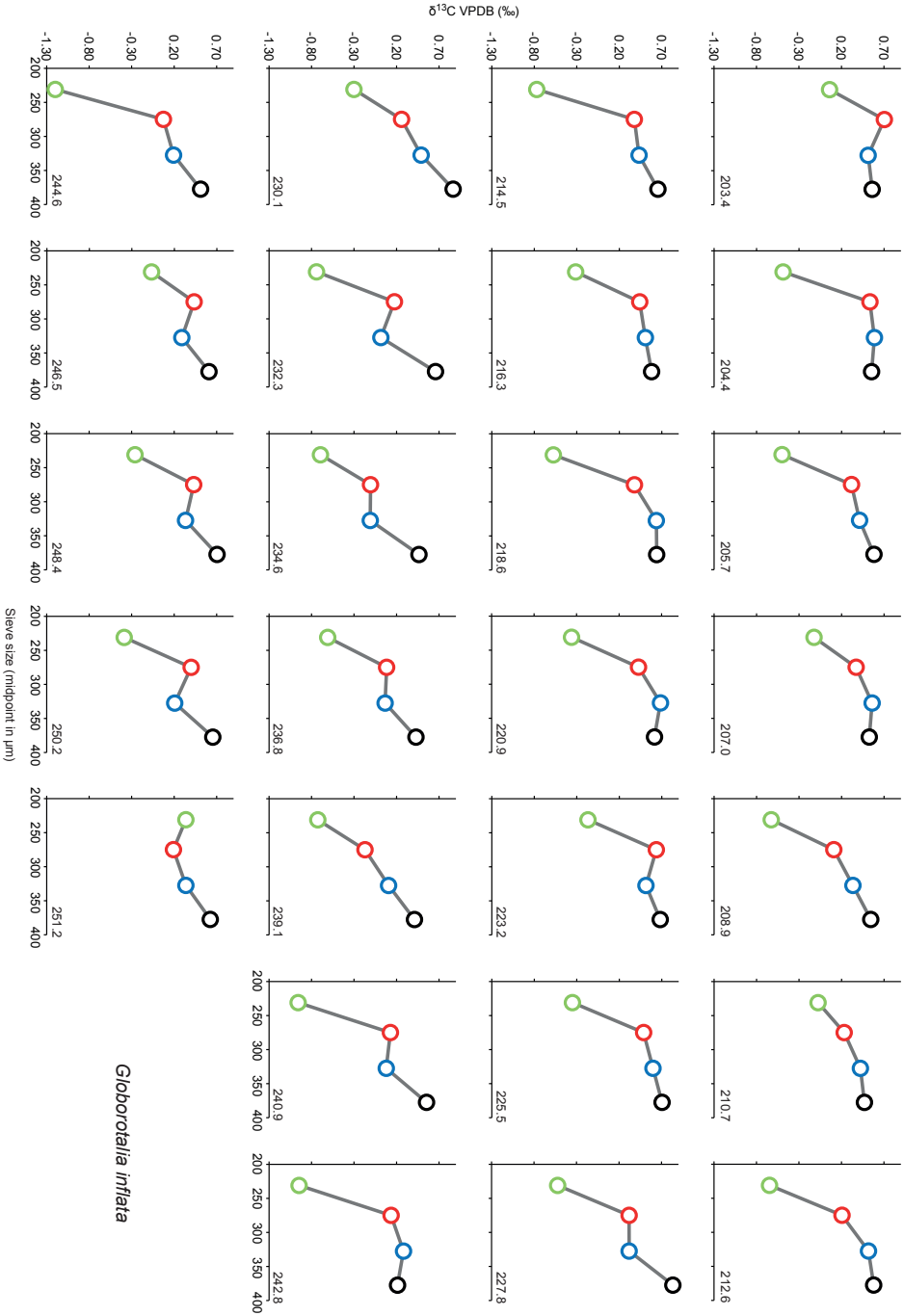




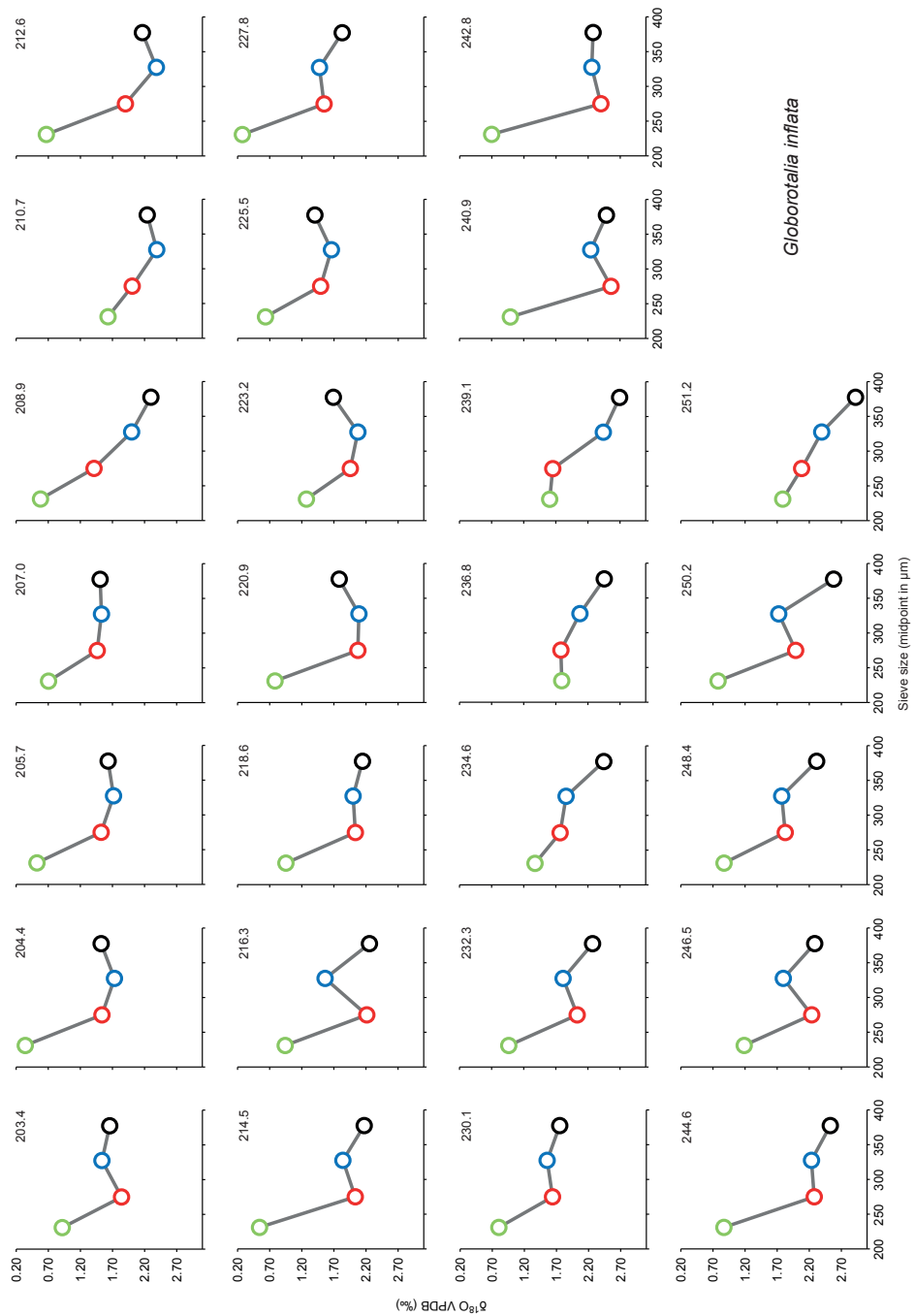
Supplementary Figure 8.1-8.6. Size isotope distribution. Intra-species size isotope distribution per sample (age in kyr in top right of plot), trends can be grouped into either: “normal” in which progressively larger sizes are more enriched, “reversed” in which larger sizes are more depleted and “mixed” in which no clear trend can be deduced, for both  $\delta^{18}\text{O}$  and  $\delta^{13}\text{C}$  [Berger *et al.*, 1978].



Supplementary Figure 8.2

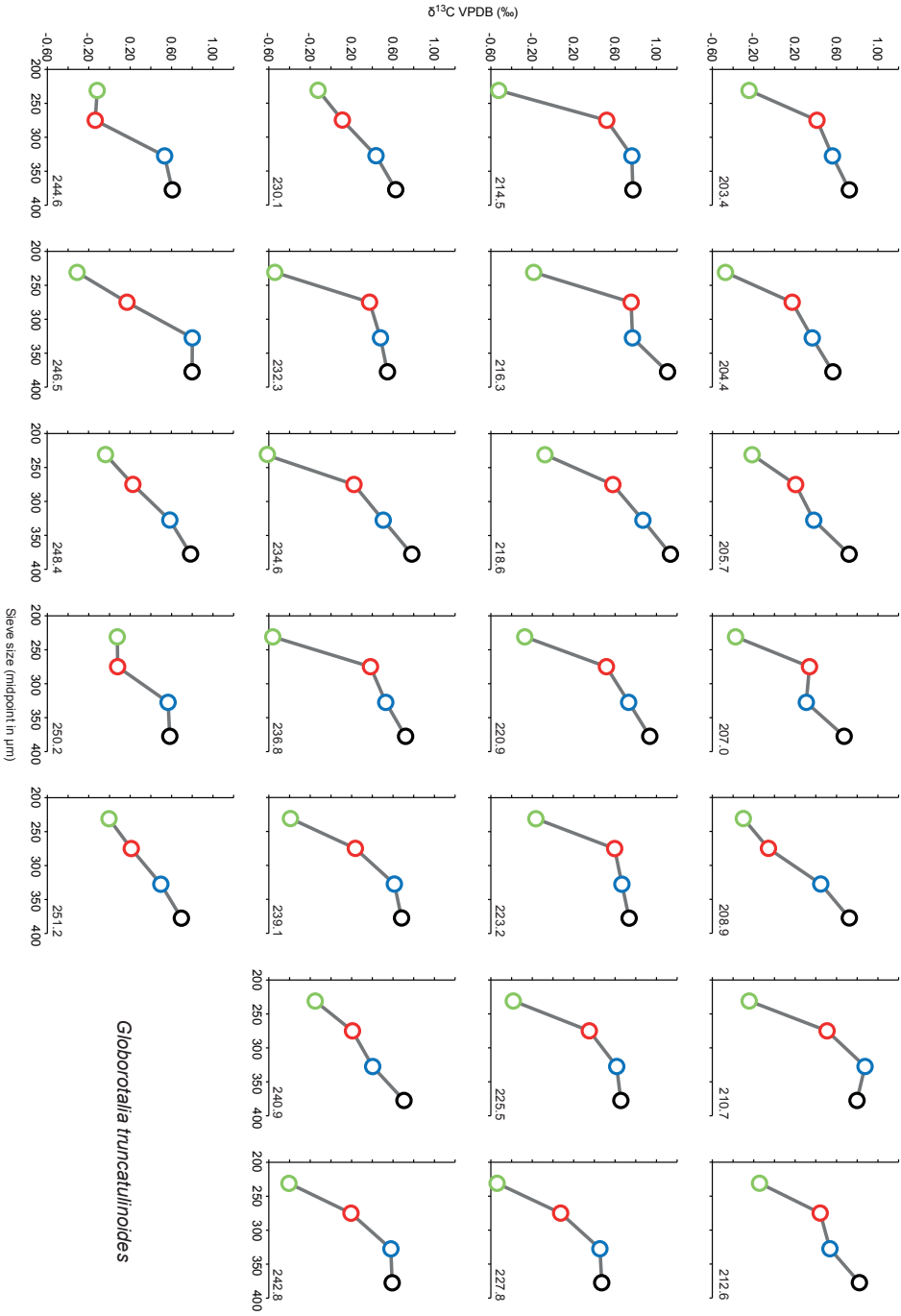


Supplementary Figure 8.3

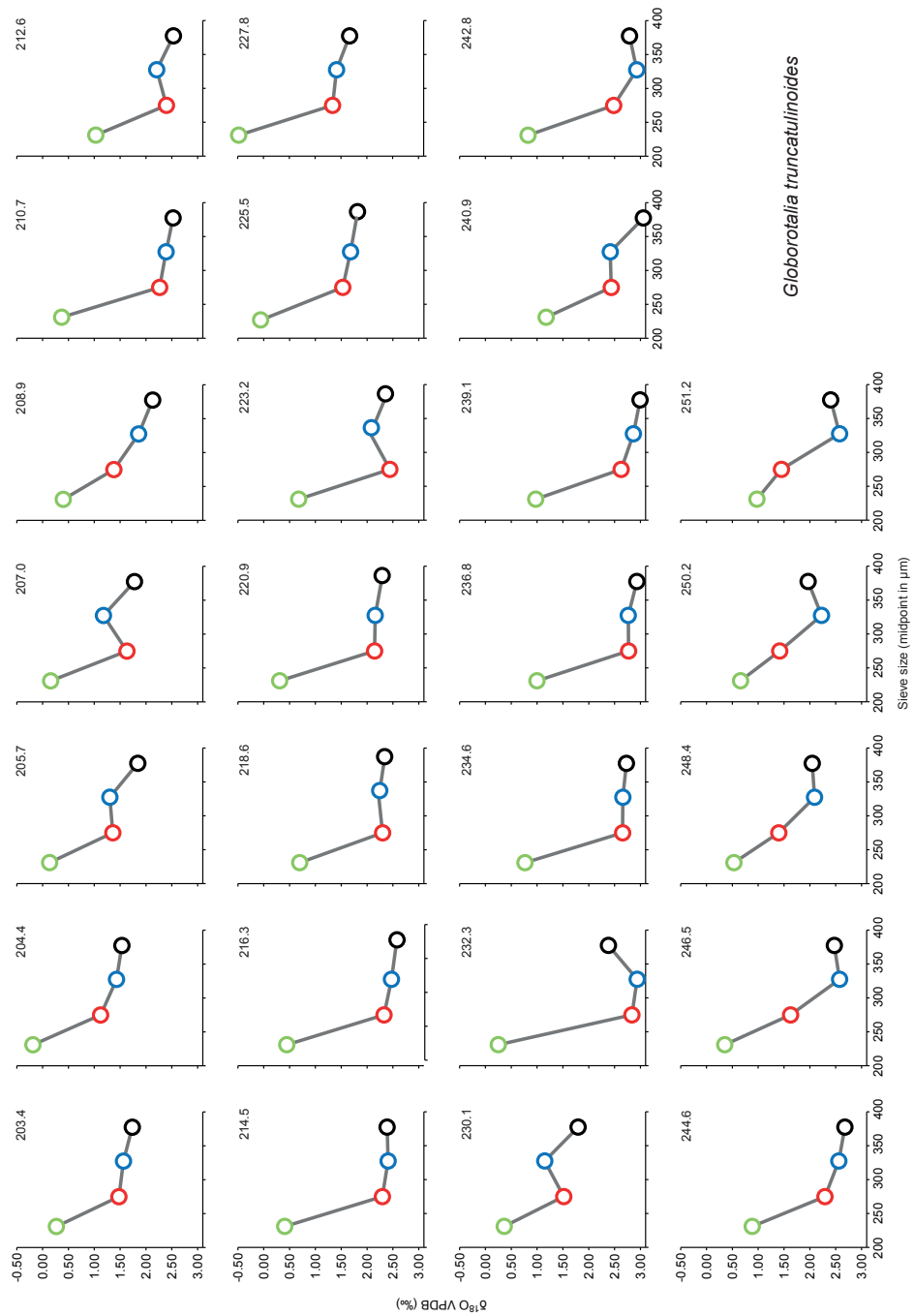


Supplementary Figure 8.4



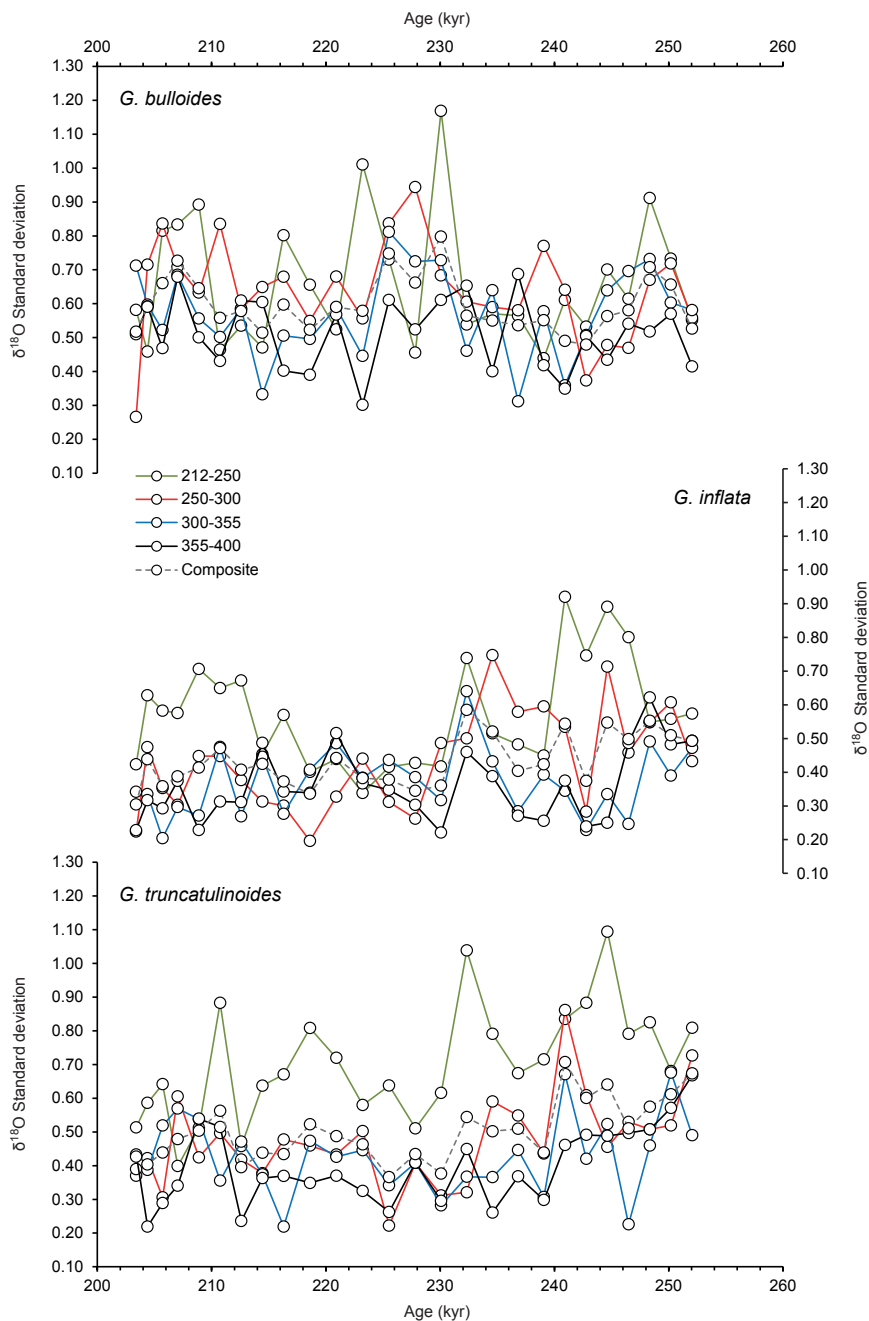


Supplementary Figure 8.5

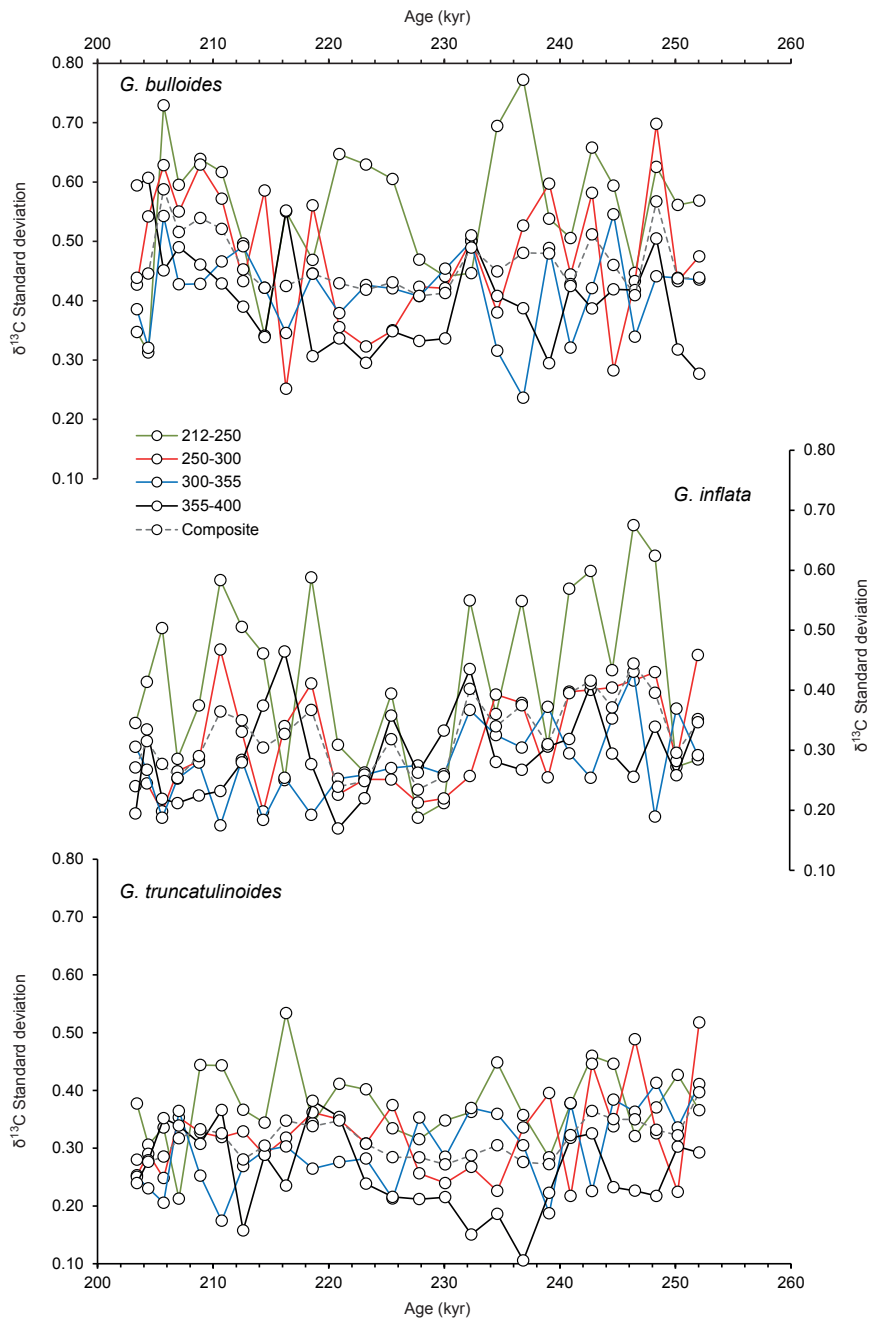


R & A

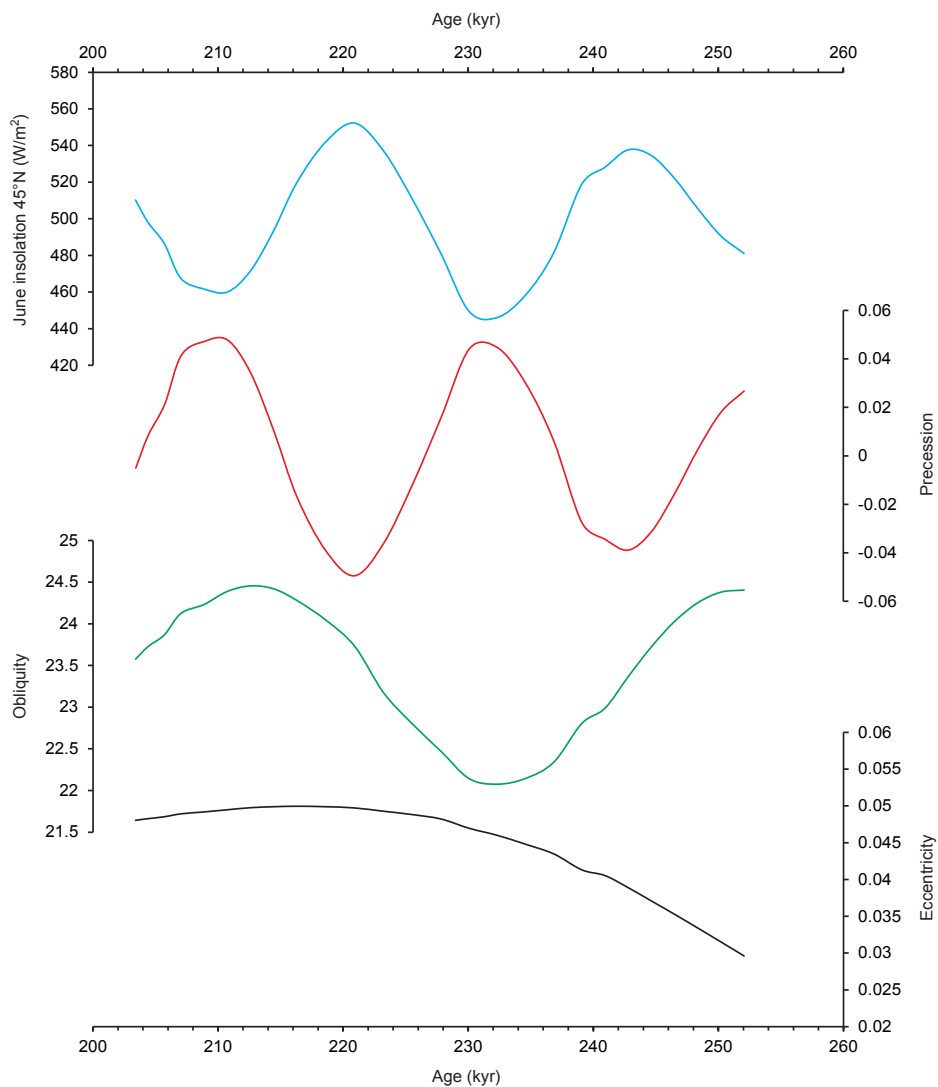
Supplementary Figure 8.6



Supplementary Figure 8.7. Standard deviation of oxygen isotopes. Standard deviation of  $\delta^{18}\text{O}$ , corrected for outliers for the analysed species *G. bulloides*, *G. inflata* and *G. truncatulinoides* for each size fraction, and the average standard deviation for all size fractions (“composite”).



Supplementary Figure 8.8. Standard deviation of carbon isotopes. Standard deviation of  $\delta^{13}\text{C}$ , corrected for outliers for the analysed species *G. bulloides*, *G. inflata* and *G. truncatulinoides* for each size fraction, and the average standard deviation for all size fractions ("composite").



Supplementary Figure 8.9. Orbital parameters during MIS8-MIS7. Computed values of June 45°N Insolation, Precession, Obliquity and Eccentricity for the time interval 200-260 kyr.



---

R & A

---